This document is confidential and is proprietary to the American Chemical Society and its authors. Do not copy or disclose without written permission. If you have received this item in error, notify the sender and delete all copies.

Mesoporous Silica Nanoparticles with pH – Sensitive Nanovalves for Delivery of Moxifloxacin Provide Improved Treatment of Lethal Pneumonic Tularemia

Journal:	*ACS Nano*
Manuscript ID	nn-2015-04306s.R1
Manuscript Type:	Article
Date Submitted by the Author:	n/a
Complete List of Authors:	Li, Zilu; University of California, Los Angeles, Department of Materials Science and Engineering Clemens, Daniel; University of California, Los Angeles, Department of Medicine Lee, Bai-Yu; University of California, Los Angeles, Department of Medicine Dillon, Barbara; UCLA, Department of Medicine Horwitz, Marcus; UCLA, Medicine Zink, Jeffrey; UCLA, Chemistry and Biochemistry

SCHOLARONE™
Manuscripts

Mesoporous Silica Nanoparticles with pH – Sensitive Nanovalves for Delivery of Moxifloxacin Provide Improved Treatment of Lethal Pneumonic Tularemia

Zilu Li[1,3,#], *Daniel L. Clemens*[2,#], *Bai-Yu Lee*[2,#], *Barbara Jane Dillon*[2], *Marcus A. Horwitz*[2,*]

Jeffrey I. Zink[3,4,*]

[1]Department of Materials Science and Engineering

[2]Division of Infectious Diseases, Department of Medicine

[3]Department of Chemistry & Biochemistry

[4]California NanoSystems Institute,

University of California, Los Angeles, California, USA

[#] Z. Li, D. L. Clemens, and B.-Y. Lee contributed equally

Address correspondence to Marcus A. Horwitz, Dept. of Medicine, CHS 37-121, UCLA School of Medicine, 10833 Le Conte Ave., Los Angeles, CA 90095-1688, USA. Phone: (310) 206-0074; Fax: (310) 794-7156; E-mail: mhorwitz@mednet.ucla.edu. or to Jeffrey I. Zink, Dept. of Chemistry and Biochemistry, UCLA, 3013 Young Dr. East, Los Angeles, CA 90095-1569, USA. Phone: (310) 825-1001; Fax: (310) 825-4911; E-mail: jiz@chem.ucla.edu.

Conflict of interest: The authors have declared that no conflict of interest exists.

ABSTRACT

We have optimized mesoporous silica nanoparticles (MSNs) functionalized with pH-sensitive nanovalves for the delivery of the broad spectrum fluoroquinolone, moxifloxacin (MXF), and demonstrated its efficacy in treating *Francisella tularensis* infections both *in vitro* and *in vivo*. We compared two different nanovalve systems, positive and negative charge modifications of the mesopores, and different loading conditions – varying pH, cargo concentration, and duration of loading – and identified conditions that maximize both the uptake and release capacity of MXF by MSNs. We have demonstrated in macrophage cell culture that the MSN-MXF delivery platform is highly effective in killing *F. tularensis* in infected macrophages, and in a mouse model of lethal pneumonic tularemia, we have shown that the drug-loaded MSNs are much more effective in killing *F. tularensis* than an equivalent amount of free MXF.

KEYWORDS: Mesoporous silica nanoparticle, optimization of uptake and release capacities, pH-sensitive nanovalve, intracellular bacteria, tularemia, *Francisella tularensis*, efficacy

ABBREVIATIONS

MSNs, mesoporous silica nanoparticles; MXF: moxifloxacin; ANA, anilinoalkane; MBI, 1-methyl-1-H-Benzimidazole; CD, cyclodextrin

Francisella tularensis is a facultative intracellular bacterial pathogen that causes tularemia, a serious and potentially fatal disease.[1] Because *F. tularensis* has extraordinarily high infectivity, causes serious morbidity and mortality, is readily cultured on a large scale, is relatively easily dispersed, and was developed as a biological weapon during World War II by Japan and in the Cold War by both the U.S. and the former Soviet Union,[2-4] it is classified as a Tier 1 Select Agent. Pneumonic tularemia, the type of tularemia of greatest concern in a bioterrorist attack, has a very high morbidity with at least half the patients requiring hospitalization, and can be fatal, resolve slowly[5] or relapse[6] even in a setting where awareness is high and appropriate treatment is available. Therefore modalities allowing more effective and rapid treatment of tularemia are needed. Nanoparticles are attractive as drug delivery platforms for tularemia treatment because the nanoparticles are avidly taken up by cells of the mononuclear phagocyte (reticuloendothelial) system - such cells are the primary host cells in which *F. tularensis* resides and multiplies. By releasing high concentrations of antibiotic in the host cells that are infected by *F. tularensis*, nanoparticles have the potential to have a greater efficacy than free drug while simultaneously limiting off-target toxicities. Nanoparticle delivery platforms also have the advantage of shielding the drug from metabolism and clearance, thereby providing more favorable pharmacokinetics than free drug.

Considerable research has been devoted to the use of MSNs for delivery of chemotherapeutic agents for cancer; relatively less has been devoted to their use for treating infectious diseases. In the case of nanotherapeutics for cancer, uptake by macrophages is a problem to be overcome. In contrast, for infectious diseases caused by pathogens that reside and multiply within macrophages, such as *F. tularensis*, the fact that the host mononuclear phagocytes internalize nanoparticles more efficiently than other cells provides an advantageous

targeting strategy with potential to increase efficacy and decrease systemic toxicities. Intravenously injected nanoparticles, or nanoparticles delivered by other routes of administration, are preferentially taken up by macrophages of the mononuclear phagocyte system and accumulate in liver, spleen and lung,[7-9] a distribution that mirrors the tissues infected by *F. tularensis* and many other important intracellular pathogens that cause serious human diseases, including those that cause tuberculosis, Legionnaires' disease, Q-fever, Salmonellosis, Listeriosis, Leishmaniasis, and chlamydial, mycoplasmal, and rickettsial infections.

Mesoporous silica nanoparticles (MSNs) offer a biocompatible multifunctional platform with intrinsically high surface area and porosity capable of delivering chemotherapeutic agents and antibiotics.[10-13] MSNs readily accommodate stimulus-responsive functionalizations to enable on-command release of drug cargo in response to a variety of stimuli, including pH,[14-17] light,[18] and remote magnetic actuation,[19] and have shown superiority over free drug both in cell culture,[20-22] and in animal models.[23] An important parameter that influences the amount of MSNs that must be administered to animals or humans for therapeutic efficacy is the "release capacity", defined as the ratio between the masses of releasable drug and of silica. The uptake and release capacity of a MSN platform depends on the properties of both the nanoparticles and the cargo molecules, including the cargo molecule size, charge in various solutions, and hydrophilic/hydrophobic properties. Herein we have systematically optimized moxifloxacin (MXF) loading of MSNs functionalized with pH sensitive nanovalves. We have studied two different pH sensitive nanovalve systems, both of which remain closed at the pH of blood (7.4) but open at pH 6 or lower and release cargo within endosomal compartments, which acidify to pH ~5 or less. We chose the most promising MSN-nanovalve platform for further optimizations based upon physical and chemical properties of MSNs and MXF.

Here, we report the optimization of our MSNs functionalized with pH-sensitive nanovalves for delivery of the fluoroquinolone antibiotic MXF, which has been shown to be more effective than Ciprofloxacin at preventing relapse of tularemia in a mouse model.[24] We demonstrate that our optimized delivery platform, MSN-MBI-MXF, is safe *in vivo* and much more efficacious than an equivalent amount of free drug in treating *F. tularensis* infection in a mouse model of pneumonic tularemia.

RESULTS AND DISCUSSION

Construction of Two pH-sensitive Nanovalve Systems

We have previously developed two pH-sensitive nanovalve systems based on the MCM-41 framework.[15, 25] Both nanovalves consist of a stalk covalently attached to the pore entrances of MCM-41 and a cap molecule cyclodextrin (CD), which interacts with the organic moiety of the stalk through hydrophobic-hydrophobic interaction and traps the cargo inside the pores. The first nanovalve is composed of an anilinoalkane (ANA) stalk and α-CD as the capping molecule. The pK_a of the nitrogen of p-anisidine is approximately 6, and at pH 7.4 the binding affinity between α-CD and the hydrophobic stalk is high. When the stalk is protonated the binding constant dramatically decreases, thereby causing the α-CD cap to dissociate from the stalk and the cargo to be released. The second nanovalve system has a 1-methyl-1-H-benzimidazole (MBI) stalk with pK_a about 6, and β-CD as the capping molecule because of its suitable cavity size and stable association with the benzimidazole moiety at physiological pH 7.4 (Figure 1). When benzimidazole is protonated at pH 6 or lower, the binding affinity between benzimidazole and β-CD decreases, leading to dissociation of the cyclodextrin. Both nanovalves are closed tightly at physiological pH 7.4 and only open and release cargo at pH 6 and lower when the hydrophobic interaction between cyclodextrin and the organic stalk moiety is weakened and interrupted.

After the stalks were attached to MCM-41, the MSN-ANA and MSN-MBI nanoparticles were loaded in MXF aqueous/PBS solution overnight and then the α-CD or β-CD capping molecule, respectively, was added to the mixture with stirring overnight. The MXF solution concentrations before and after loading were measured and calculated based on UV-Vis spectroscopy measurements. The amount of MXF taken up by the MSNs (including inside pore channels and

on external surfaces) was calculated from this concentration difference. The mass of MXF taken up by the MSNs divided by their mass is defined as "uptake capacity" (expressed in wt %). After washing the mechanized MSNs sufficiently to remove MXF on the outer surface, the nanoparticles were dispersed in neutral water, and then acid was added to decrease the pH and release the drug (Figure 2A). When MSNs were placed at the corner of a cuvette in neutral solution, no MXF was detected in the supernatant fluid by fluorescence measurement. When the solution pH was adjusted to 6 by adding HCl, immediate release of MXF was observed (Figure 2B and S1). It is known that the pH within the lysosome is lower than 6; thus, the nanoparticles should release the drug after being endocytosed into the lysosome compartment. This drug would then be available to diffuse to *F. tularensis*, which resides and replicates in the cytosol of the cell,[26] where the pH is neutral. The amount of MXF released was calculated based on the supernatant MXF concentration measured by UV-Vis. The mass of released MXF divided by the mass of particle is defined as "release capacity" (expressed in wt %). The porous structure is preserved after these modifications (Figure 2C) and the hydrodynamic diameter is around 100 nm (Figure S2).

Enhancement of Uptake Capacity by Charge Modification of the Mesopore Channels

To optimize the uptake and release capacities, we must consider five relevant factors: charges of cargo molecules and MCM-41 inner pore channels, nanovalve synthesis pathway, loading solvent pH, MXF concentration and loading time. MSNs with the MBI stalks (MSN-MBI) were selected as the initial model; when investigating the effects of one factor on the uptake and release capacities, all of the other parameters were kept constant.

MXF is a fourth generation fluoroquinolone used to treat various bacterial infections including *F. tularensis*. It has two ionizable groups with pK_a of 6.3 and 9.3. Based on the calculation of the molecular species distribution, at pH 7, 83.3% of MXF molecules are zwitterionic, 17% are positively charged, and almost none are negatively charged (Table 1). MXF has a positive net charge at neutral pH. A negatively modified inner pore readily attracts positive cargo molecules, but the release may be slow and incomplete after the cap dissociates due to the electrostatic interaction between cargo molecules and inner pores at the pH of acidifying endosomal compartments.[27] On the other hand, a positively charged inner pore surface will lead to lower uptake capacity than when negatively charged but may promote expulsion of the positive cargo molecules upon protonation. To modify the MSN inner pores with either negative or positive charges, we synthesized MCM-41 with co-condensation of phosphonate or amine silanes respectively (Figure 3A). Phosphonate silane-modified MSNs exhibited a zeta potential of -46.28 mV and amine-silane modified MSNs exhibited a zeta potential of 38.76 mV as measured in DI water. MSN-MBI (10 mg) was dispersed in 2 ml of a 5 mM MXF aqueous solution and uptake capacity was measured as described above. Amine modified MSN-MBI (indicated as "+") had a very low uptake capacity compared with that of phosphonate modified MSN-MBI (indicated as "-") (Figure 3B). This result indicates that MXF with a positive net charge diffuses poorly into positively charged inner mesopores, resulting in very low uptake and release capacities. Phosphonated particles, on the other hand, show much greater uptake of MXF, potentially providing a much greater release capacity.

We next tested two different MBI stalk synthetic pathways to optimize the efficiency of attachment. In the first pathway, we first reacted benzimidazole with chloromethyltrimethoxysilane to produce the MBI stalk, and then covalently attached this to the

MCM-41 surface. This method has the disadvantage that, in the presence of small amounts of water or moisture, the MBI stalk readily hydrolyses and undergoes self-condensation prior to coupling to the nanoparticle. In the second pathway, we covalently attached chloromethyltrimethoxysilane to the silica surface first and then coupled it with benzimidazole to form the MBI stalk. We compared the uptake capacities of negatively charged MSN-MBI nanoparticles prepared by these two pathways and found that MBI stalk attachment by pathway II had a higher uptake capacity than attachment by pathway I, consistent with greater MSN surface coverage by the MBI stalks and hence greater trapping of drug in the pore channels.

Uptake and Release Capacity Utilizing Different Nanovalves

Both MSN-ANA and MSN-MBI were tested and proven to work effectively in our previous papers when loaded with doxorubicin, Hoechst 33342, or propidium iodide (PI).[15, 25] However, we know that the uptake capacity and release capacity of the MCM-41 nanovalve system is dependent upon the size and charge of the cargo molecule, as well as the length of the stalk and the outer diameter of the CD. We measured and compared the uptake capacity of MXF utilizing these two systems in order to find the best one for subsequent *in vitro* and *in vivo* studies.

Because negatively charged inner pores provided greater uptake of MXF, we used phosphonated MCM-41 and compared the uptake and release of MXF of MSN-ANA-MXF, which has α-CD as cap, and MSN-MBI-MXF which has β-CD as cap. The same amount of phosphonated MCM-41 with one or the other nanovalve was loaded in 1 ml 10 mM MXF PBS solutions and stirred for one day. MSN-MBI-MXF had a much higher uptake capacity (7.4 wt%) and release capacity (1.02 wt%) than MSN-ANA-MXF (Table 2). The superior uptake and release capacity of the MSN-MBI-MXF is likely attributable to better trapping of the MXF within the pores. The β-CD

has a 15.6 Å outer diameter compared with 14.6 Å for α-CD while MCM-41 has an average pore diameter of 22 Å.[15] The larger β-CD has more steric hindrance and blocks the MSN pores more effectively than the smaller α-CD. Moreover MSN-MBI has a shorter stalk length that positions the β-CD cap closer to the MSN surface, again providing more effective steric hindrance to prevent MXF leakage. For both types of MSNs, the uptake capacity was greater than the release capacity in aqueous acid, indicating that some MXF remains bound to the MSNs and is not released in aqueous acid conditions, possibly reflecting binding of MXF to MSN *via* hydrophobic interactions.

Uptake of MSN with pH Sensitive Nanovalves by Human Macrophages

Nanoparticles are generally taken up well by cells of the mononuclear phagocyte system and, where this is not desired, require special surface modifications to minimize their uptake by macrophages in applications such as cancer therapeutics.[28] However, in our system, uptake by macrophages is desired, since *F. tularensis* replicates in host mononuclear phagocytic cells. Our MSN platform is designed to operate by uptake of the particles by macrophages, followed by release of drug within acidified endo-lysosomal compartments. To determine whether our MSNs are internalized by *F. tularensis*-infected macrophages, we examined the uptake of rhodamine-labeled MSNs by *F. tularensis*-infected human macrophages, using both peripheral blood monocyte-derived macrophages (Figure S3) and differentiated macrophage-like THP-1 cells. We observed abundant uptake of MSN-MBI-MXF for both the monocyte-derived macrophages and the differentiated THP-1 cells (Figure 4). Uptake of the nanoparticles by both types of macrophages increased with time and with nanoparticle concentration (Fig. S4).

In Vitro Efficacy of MSN-ANA-MXF and MSN-MBI-MXF in Killing *F. tularensis* in Human Macrophages.

To investigate whether these two different types of pH-sensitive α- and β-CD nanovalves are functional under biological conditions, we assessed the efficacy of MSN-ANA-MXF and MSN-MBI-MXF in a macrophage infection model of *F. tularensis*.[29] Differentiated human THP-1 macrophages were infected with *F. tularensis* Live Vaccine Strain (LVS) and either not treated or treated with increasing concentrations of a) MXF, b) MSN-ANA-MXF, or c) MSN-MBI-MXF for one day. At the end of the treatment period, the number of viable bacteria remaining in the macrophages was determined to evaluate the *F. tularensis* killing effect exerted by each treatment. With no treatment, *F. tularensis* LVS grew 2.5 logs over one day. Similar levels of bacterial growth were also observed in infected macrophages treated with control MSNs (no MXF loading) indicating that the nanoparticle carriers alone do not possess any bactericidal activity (Figure 5B and C). All treatments including MXF, MSN-ANA-MXF and MSN-MBI-MXF killed *F. tularensis* in macrophages in a dose- dependent manner (Figure 5A, B and C). However, when compared at the same concentration, MSN-MBI-MXF was much more potent than MSN-ANA-MXF in killing *F. tularensis*. For example, MSN-MBI-MXF at 1 μg/mL reduced bacterial colony forming units (CFU) by 3.4 logs compared with the level in the untreated group at one day, whereas the same concentration of MSN-ANA-MXF reduced bacterial CFU by only 0.2 logs compared with the untreated control group. The minimal inhibitory concentration in our macrophage assay is 4 μg/mL for MSN-ANA-MXF and it falls to between 0.25 and 0.5 μg/mL for MSN-MBI-MXF (Table S1).

We prepared supernate from MSN-ANA-MXF and MSN-MBI-MXF after an hour of incubation with 100 mM maleic acid, pH 1.8 (Acid Release) and assayed its capacity to kill *F. tularensis* in

the infected macrophage. While the acid-released solution prepared from 0.5 and 1 μg/mL MSN-MBI-MXF reduced *F. tularensis* CFU in macrophages by 1.6 and 2.5 logs, respectively, the solution prepared from 1 μg/mL of MSN-ANA-MXF reduced bacterial number by only 0.2 logs (Figure 5D and E). Supernates obtained from MSN-MBI-MXF or MSN-ANA-MXF at neutral pH (Neutral Eluate) had no effect in the infected macrophage bioassay. This study demonstrates that 1) the pH operative valves on MSN-MBI-MXF are tightly closed at neutral pH and open at acidic pH, 2) MXF eluted under acidic pH retains biological activity, 3) MSN-ANA-MXF and MSN-MBI-MXF kill *F. tularensis* LVS in macrophages in a dose-dependent fashion, and 4) MSN-MBI-MXF has greater efficacy than MSN-ANA-MXF, most likely because of its higher MXF uptake and release properties.

Acid-released solution obtained from 1 μg/mL of MSN-MBI-MXF exerted the same inhibitory effect on *F. tularensis* as 0.016 μg/mL MXF in our macrophage bioassay, indicating a 1.6% (wt/wt) aqueous acid release capacity. Based on this estimation, 0.5 μg/mL of MSN-MBI-MXF could release 0.008 μg of MXF in the acidified endolysosomes. In our *F. tularensis*-infected macrophage assay, MSN-MBI-MXF at 0.5 μg/mL had a biological effect equivalent to that exerted by free MXF at a concentration of 0.016 μg/mL, indicating an efficacy ratio of 2 (MSN-MBI-MXF : free MXF), as nanoparticle-delivered drug appeared to have an efficacy twice that of the same amount of free drug in killing *F. tularensis* in macrophages *in vitro*. However, this efficacy ratio is likely an over-estimation since some of the yellowish color of MXF still remained on MSN-MBI-MXF after maleate treatment. In lieu of a possible hydrophobic interaction between MXF and MSN, we used acidic DMSO solution for measuring drug release capacity in subsequent *in vivo* studies.

Maximization of Uptake and Release Capacity by Optimization of Loading pH

Our *in vitro* study indicated that it is important to obtain a high release capacity in order to achieve high efficacy. Therefore we sought to increase further the uptake and release capacities of MSN-MBI-MXF.

Specifically, we prepared MXF in different pH solutions for use in the loading process to take advantage of electrostatic interactions based on positively or negatively charged inner pore channels. It is known that MXF has a positive net charge below pH 7.4 and negative net charge above pH 7.4 (Table 1). Therefore we loaded phosphonate modified MSN-MBI (10 mg) (indicated as "-") in pH 4 and pH 7 MXF solution (5 mM, 2 ml) in order to attract positive MXF molecules and increase uptake capacity. However, this acid loading presents some practical problems in experiments. The pH 4 loading helps improve uptake capacity as expected. However, it results in lower release capacity than neutral loading. Because the nanovalve can open at pH 6, loaded MSN-MBI must be transferred to neutral solution before capping. The additional steps of centrifugation and dispersion of uncapped MSN-MBI-MXF in neutral water cause significant leakage of MXF from the particle pores before capping can be completed. We loaded amine modified MSN-MBI (10 mg) (indicated as "+") in pH 7, 10, and 12 MXF solutions (5 mM, 2 ml) to attract negative MXF molecules. We observed that uptake capacities as well as release capacities increased as pH was increased (Figure 6). Among these five conditions of loading, amine modified MSN-MBI in pH 12 loading gave the highest uptake capacity; however, the release capacity was still no better than pH 7 loading with phosphonate modified MSN-MBI. Using a pH 12 loading solution may gradually degrade the MSNs within 24 hours and cause stalks to detach from the pores, enabling MXF to leak out of the pores during washing.

We found that loading phosphonated MSN-MBI with MXF in pH 7.4 PBS yielded the highest uptake and release capacity among all conditions (Figure 7). When phosphonate modified MSN-

MBI (10 mg) was loaded in 1 ml 20 mM MXF in PBS (pH 7.4), its uptake capacity increased more than 10 times compared with its loading in neutral solution. Considering stalk protonation and deprotonation equilibrium, MSN-MBI is more tightly closed with β-CD at pH 7.4 than it is at pH 7. Negatively charged mesopores also have strong electrostatic interaction with positive MXF molecules. Moreover, compared with strong base, the pH 7.4 loading solution will not cause hydrolysis of silica nanoparticles and degradation of the nanovalves attached at the entrances of pore channels. All of these factors contribute to the highest uptake capacity.

We have found that a higher MXF loading concentration resulted in a higher uptake and release capacity. MSN-MBI loaded with 40 mM MXF in PBS had an uptake capacity twice that of MSN-MBI loaded with 20 mM MXF in PBS, and the release capacity reached 8.1 wt% compared with 6.2 wt% for MSN-MBI loaded with 20 mM MXF. Moreover, when we compared uptake efficiency, which is defined as the percentage of MXF taken up by MSN from the original solution (expressed in percent), almost 70% of MXF in high concentration solution was taken up by nanoparticles. We also observed that a loading time of 24 hours was appropriate to allow MXF to diffuse into pore channels and reach equilibrium. Simply extending loading time did not increase uptake and release capacity (Figure S5). We tested phosphonated MSNs modified with two different nanovalves (ANA, MBI); the MSNs were loaded in MXF in PBS at low concentration (10mM) and washed extensively with PBS buffer. The MSN-ANA and MSN-MBI showed uptake and release capacities of 20 wt% / 0.24 wt% and 51.4 wt% / 1.6 wt%, respectively; therefore MSN-MBI still showed the best performance in the final optimized condition (Table 3). In conclusion, phosphonated MSN-MBI loaded with MXF in PBS showed the highest release capacity, 6 – 8 wt%, among all systems tested; this was highly reproducible

and this MSN loaded with MXF in PBS was employed in subsequent *F. tularensis in vitro* and *in vivo* studies.

Influence of Washing on Release Capacity

In the washing process, the mass of MXF washed away each time divided by the mass of particle is defined as "residual" (expressed in wt %), of which the final residual is reflected as the starting baseline in a release profile. Through measurement by UV-Vis spectroscopy, the amount of residual drug in supernatant did not increase after dispersing and rotating particles in neutral water overnight, which indicated that the residual was not due to release or leakage, but caused by non-trapped MXF dissociating from the MSN-MBI-MXF surface. In the release process, we dispersed particles in neutral deionized water and observed no leakage from MSN-MBI as indicated by the flat baseline in the release profile. After adding HCl to adjust the pH to 5, we measured an immediate increase in fluorescence intensity from the MXF released into the supernatant. The release profile reached a plateau after 14 hours, and the concentration of completely released MXF was measured by UV-Vis spectroscopy after 24 hours.

We investigated how the washing process influences particle release capacity. In testing drug-loaded nanoparticles, we routinely wash them to remove free MXF adsorbed on the external surface of the MSN to insure that the great majority of the drug is released *via* the nanovalves. However, excess washing will gradually degrade the silica nanoparticle surface due to siloxane group hydrolysis. Moreover, it will remove some of the cyclodextrin caps by disrupting host-guest interaction equilibrium. Therefore, it is important to determine the optimal number of washing steps that strikes an acceptable balance between removing MXF from the external surface and maintaining relatively high release capacity. MSNs washed 15 times did not have

any residual surface MXF detectable by UV-Vis absorption measurement (Figure 8A); however, their release capacity was only 1.6 wt%. In contrast, MSNs washed 8 times had 2.5 wt% residual and 6.9 wt% release capacity. MSN-MBI-MXF washed 21 times had almost zero residual in the last few washes. There is an non-linear decay of the amount of MXF washed away each time, with the first 8 washes removing around 95 % of the total amount of MXF (Figure 8B). We found that washing 8 times is enough to remove most of the MXF on the MSN external surface and at the same time constrain damage to surface modifications.

In Vivo Efficacy of MSN-MBI-MXF in Treating Pneumonic Tularemia

It is important to test nanoparticle delivery systems *in vivo* as well as *in vitro*. Nanoparticles that are effective in an *in vitro* system may fail in an *in vivo* model due to issues of efficacy, such as inadequate uptake by target organs or premature release of drug, and issues of toxicity, e.g. due to induction of coagulopathy,[30] hemolysis,[31] organ toxicities or inflammatory responses.[32] After the above optimizations of our MSNs so as to achieve high uptake and release capacity, we assessed the efficacy of MSN-MBI-MXF in a mouse model of pneumonic tularemia.[33, 34] In the first *in vivo* experiment (Experiment 1), mice were infected by the intranasal route with ~8000 CFU of *F. tularensis* LVS, a dose approximately 11 times the LD_{50} of 700 CFU. Without treatment, the mice succumbed rapidly to the infection and suffered severe weight loss (Figure 9A). Mice treated with MSN-MBI-MXF (with a drug release capacity of 6.88 wt%) maintained their weight, indicating that the nanoparticle was well tolerated by the mice and helped to control the severe bacterial infection. Without treatment, bacteria multiplied to high numbers in the lungs of the mice (Figure 10A). However, treatment with MSN-MBI-MXF (loaded with 138 μg MXF) reduced bacterial burden in the lung by 4.0-logs, more so than treatment with 400 μg of free MXF (Figure 10C). Treatment with MSN-MBS-MXF reduced bacterial burden in the spleen

by 4.3-logs to a level similar to that with 400 μg of free MXF which was below our experimental limit of detection. All treatments reduced bacterial burden in the liver to a level below the experimental detection limit. On the basis of a median-effect plot, the efficacy of the MSN-MBI-MXF was 4.5 fold and 3 fold the efficacy of free MXF in the lung and spleen, respectively (Figure S6, left panel). This study demonstrates that MSN-MBI-MXF administered intravenously is much more efficacious than free MXF in treating *F. tularensis* infection in mice.

In a subsequent *in vivo* experiment (Experiment 2), we evaluated another batch of MSN-MBI-MXF (with a drug release capacity of 8.08 wt%). Mice were infected with ~4000 CFU of *F. tularensis* LVS (~6 x LD_{50}) by the intranasal route. One day later, mice were sham-treated or treated with 640 μg of MSN-MBI-MXF (with ~ 50 μg of releasable MXF) or with one of the three doses of MXF (50, 100, and 200 μg) equal to 1x, 2x, and 4x the amount of the releasable MXF from 640 μg of MSN-MBI-MXF by acidic DMSO. As observed in the first *in vivo* study, sham treated mice suffered substantial weight loss but mice treated with free MXF or MSN-MBI-MXF did not (Figure 9B). MSN-MBI-MXF treatment reduced the bacterial burden by 2.8 logs in the lung, 3.2 logs in the liver, and 3.3 logs in the spleen to a level close to that achieved by 100 μg free MXF (Figure 10D). Thus, in the treatment of pneumonic tularemia in mice, MSN-MBI-MXF had an efficacy twice the equivalent amount of free MXF in the lung, spleen, and liver (Table S2 and Figure S6, right panel). Again, we observed no toxicity in the mice from MSN-MBI-MXF treatment. Thus, these two experiments both demonstrated superiority of MSN-MBI-MXF over an equivalent amount of free MXF. In the first experiment, bacterial CFU were reduced in the lungs compared with that achieved by free drug, and the difference was statistically significant; comparisons in liver and spleen could not be made because sterilization was achieved at the doses used for all treatments. In the second experiment, we reduced the dose

of MSN-MBI-MXF to prevent “bottoming out” of the values in the liver and spleen and showed that the MSN-MBI-MXF treatment reduced bacterial CFU more than an equivalent amount of free drug in these organs, a difference that was statistically significant. Bacterial burden in the lungs was also reduced more in the MSN-MBI-MXF treated animals than in animals treated with an equivalent amount of free drug, though this trend did not reach statistical difference at this lower dose of MSN-MBI-MXF.

CONCLUSION

Intracellular pathogens that reside in mononuclear phagocytes present an ideal target for nanotherapeutics because nanoparticles are readily taken up by cells of the Mononuclear Phagocyte System and have the potential to deliver high concentrations of antibiotics selectively to the intracellular compartment, thereby providing increased efficacy with reduced systemic exposure and off-target side effects.

We have optimized MSNs with pH-sensitive nanovalves for uptake and release of the antibiotic MXF. We evaluated a) two different pH-sensitive nanovalves; b) modification of the MSN's inner pores with positive or negative charges; c) loading of the MSNs with MXF in different pH solutions; and d) loading MSNs with different drug concentrations and loading durations. We found that phosphonated MSN-MBI-MXF loaded in pH 7.4 PBS gave the highest uptake and release capacity. We demonstrated that this delivery system released MXF efficiently in *F. tularensis*-infected macrophages and that it was 2.7 fold more effective than the amount of free drug released from the particles by aqueous acid. We demonstrated in a mouse model of lethal pneumonic tularemia that MSN-MBI-MXF was well tolerated and was more effective than a 2- to 4-fold greater dose of free MXF in reducing bacterial load in the lung. Our MSN-MBI-MXF delivery system has the potential to provide more effective treatment than free drug, shortening the duration of treatment of intracellular infectious diseases such as tularemia, tuberculosis, Q-fever, and Legionnaires' disease and reducing systemic toxicity of the MXF. By providing high concentrations of antibiotic directly to the site of infection, the nanoparticle delivered drug also has the potential to decrease the emergence of drug resistance. Further optimization of our platform may be possible by incorporation of additional functionalizations to increase targeting

to infected tissues and macrophages, employment of different delivery modalities, such as aerosol delivery, or utilization of other internal and external stimulus-response systems.

METHODS

Materials. Cetyltrimethylammonium bromide (CTAB, 95%), tetraorthoethylsilicate (TEOS, 98%) 3-(trihydro-xysilyl)propyl methylphosphonate (42% in H_2O), 3-iodopropyltrimethoxysilane (IPTMS, 95%), N,N'-dimethylformamide (99.8%), p-anisidine (99%), α-cyclodextrin (≥98%), β-cyclodextrin (≥97%), benzimidazole (98%), tetrabutylammonium iodide (98%), Hoechst 33342 (≥97%), triethylamine (≥99%), and toluene (99.8%) were purchased from Sigma (St. Louis, MO). Chloromethyltrimethoxysilane (90%), and N-(2-Aminoethyl)-3-aminopropyltrimethoxysilane (NAPTS, 90 %) were purchased from Gelest (Morrisville, PA).

Synthesis of MCM-41. The synthesis of MCM-41 was based on well-established published procedures. Cetyltrimethylammonium bromide (CTAB, 250 mg, 0.7 mmol) was dissolved in H2O (120 mL) and NaOH (875 μL, 2M). The mixture was heated up to 80 °C and kept stable for 30 minutes, followed by adding tetraethyl orthosilicate (TEOS, 1.2 mL) drop-wise into the solution while stirring vigorously. For phosphonated MCM-41, 3-(trihydroxysilyl)propyl methylphosphonate (315 μL) was added into the solution 15 minutes after adding TEOS. For amine modified MCM-41, N-(2-Aminoethyl)-3-aminopropyltrimethoxysilane (90 %) was mixed with TEOS before adding to CTAB solution. The solution was kept at 80 °C for 2 hours. The synthesized nanoparticles were centrifuged and washed thoroughly with methanol. The successful synthesis of nanoparticles is very sensitive to the temperature and stirring speed.

Synthesis of Anilinoalkane (ANA) Nanovalve. As-synthesized MCM-41 (100 mg) was washed and dispersed in anhydrous toluene, mixed with 3-iodopropyl trimethoxysilane (IPTMS, 20 μL, 0.1mmol) and heated up to 40 °C under N_2 for 12 hours. The IPTMS modified nanoparticles

were washed with toluene to remove unreacted agents and re-dispersed in anhydrous toluene, and mixed with p-anisidine (123.2 mg, 1 mmol) and triethylamine (TEA, 420 μL, 3 mmol). The solution was refluxed under N_2 for another 24 hours. The final product was centrifuged and washed with toluene, methanol and water to be ready for drug/dye loading process.

Synthesis of 1-Methyl-1H-benzimidazole (MBI) Nanovalve. MCM-41 (100 mg) was washed and dispersed in anhydrous toluene, mixed with chloromethyltrimethoxysilane (15 μL) and refluxed for 12 hours. The modified MCM-41 was washed by toluene and dimethyoformamide (DMF) and dispersed in 8 ml DMF. Tetrabutyammonium iodide (2 mg), benzimidazole (12 mg) and triethylamine (150 μL) were added into the solution and the mixture was heated up to 70 °C under N_2 for 24 hours. As-synthesized nanoparticles were washed with DMF, methanol and water thoroughly.

Surfactant Template Extraction. Nanovalve-modified MCM-41 (100 mg) was dispersed in methanol (60 mL), mixed with concentrated HCl (12 M, 2.3 mL) and refluxed for 8 hours under N_2, and then washed extensively with methanol and water.

Drug Loading and Washing. 10 mg of nanovalve-modified MCM-41 was suspended in MXF PBS solution at various concentrations overnight. β-CD (40 mg) was added to the suspension and mixed for 12 hours to make sure the capping molecule reached an equilibrium with stalks on the nanoparticle surface. Loaded and capped nanoparticles (10 mg) were centrifuged down in a 2 mL tube and the supernate kept for UV-Vis absorbance measurement. Filtered PBS was added into the tube and nanoparticles were suspended and sonicated again. This washing process was repeated and the number of times the nanoparticles were washed was the same for each group being compared.

Uptake Capacity and Release Capacity Measurement. After measuring UV-Vis absorbance of MXF remaining in the PBS loading solution and of standard MXF PBS solution with known concentrations of 0.01 mM, 0.02 mM and 0.025 mM MXF, the amount of unloaded MXF concentration was calculated based on Beer's law. Uptake capacity (wt %) = [(WMXF before loading – WMXF after loading) / Wparticle)] × 100 %. In the optimization experiments, the loaded MSN-MXF particles were dispersed in pH 4.5 HCl solution for 24 hours and then centrifuged down to measure the concentration of MXF released into the supernate. Release capacity (wt %) =(Wreleased MXF / Wparticle) × 100 %. In our *in vitro* and *in vivo* studies of the efficacy of the nanoparticles in treating *F. tularensis* infection, MSN-MXF was dispersed in pH 1 HCl/DMSO solution to measure the maximum release capacity.

Stimulated Release Studies. To measure MXF release from MSNs and detect MXF fluorescence emission in supernates, dried MSN-MXF powder was put in the corner of a glass vial containing 10 mL DI water. A probe laser beam (5 mW 377 nm) was passed through the supernatant fluid in the glass vial such that released MXF was excited. The fluorescence was detected and collected by a charge-coupled device (CCD) detector and a computer at 1 s intervals over the course of the experiment. Baseline spectra were collected for 1 hour to confirm that there was no MXF leakage, and then 1 M HCl solution was added to adjust the pH to 4.5. The release profile was the plot of the integrated emission peak area between 480 nm to 520 nm as a function of time.

Physisochemical Characterization of Nanovalve Modified MSN. Transmission electron microscopy (TEM) images of MSN were obtained using a JEM1200-EX (JEOL) instrument (JEOL USA, Inc., Peabody, MA). Particle size and zeta potential were measured by ZetaSizer

Nano (Malvern Instruments Ltd, Worcestershire, UK) with 50 μg/mL MSN dispersed in DI water.

Bacteria. *F. tularensis* subsp. *holarctica* Live Vaccine Strain (LVS) was obtained from Centers for Disease Control and Prevention (Atlanta, GA). LVS glycerol stocks were prepared as described and stored at -80°C.[33] For *in vitro* macrophage experiments, a vial of the LVS frozen glycerol stock was thawed in a 37 °C water bath and cultivated on GCII chocolate agar plates for 3 days before use. For *in vivo* mouse experiments, a vial of pre-titered LVS frozen stock was used directly to infect mice and immediately afterward serially diluted and plated on GCII chocolate agar to confirm the bacterial numbers used to infect. For fluorescence studies, LVS expressing superfolder green fluorescent protein (LVS-GFP) was grown on GCII chocolate agar containing kanamycin at a concentration of 10 μg/mL for 3 days prior to use for infecting macrophages.

Macrophages. Human peripheral blood monocytes were prepared from the blood of healthy donors and cultivated in Teflon wells for 5 days to differentiate them into monocyte derived macrophages.[29] Human THP-1 monocytic cells (American Type Culture Collection, TIB-202) were maintained in RPMI-1640 (Lonza) supplemented with 10% fetal bovine serum (Mediatech), 2 mM GlutaMAX (Life Technology), penicillin (100 IU) and streptomycin (100 μg/mL) at 37 °C, 5% CO_2 – 95% air atmosphere. Prior to usage, THP-1 cells were differentiated into macrophages with 100 nM phorbol 12-myristate 13-acetate (PMA; Sigma) in antibiotic-free RPMI with 10% fetal bovine serum.

Assessment of MSN Efficacy in Macrophages. PMA-differentiated THP-1 cells were plated at 1 x 10^5 cells per 200 μL per well in 96-well plates (Matrical) and infected with 10^6 *F. tularensis*

LVS for 90 min. The infected THP-1 macrophages were washed and incubated with fresh medium alone or fresh medium containing MXF, control MSNs (no MXF loading) or MXF-loaded MSNs. *F. tularensis* LVS infection and growth in THP-1 macrophages was determined by harvesting the bacteria from the infected macrophages at 2 hours and 1 day post infection. For all treatment groups, the infected macrophage cultures were incubated in the continued presence of the treatment for one day (the free drug or nanoparticles were neither washed away nor re-added). Thereafter, *F. tularensis* LVS was harvested from the infected macrophages to assess the effect of treatment. The bacteria were harvested by lysing the macrophage monolayers with 1% saponin in PBS for 5 min at room temperature, serially diluted, and plated on GCII chocolate agar. Bacterial colony forming units (CFU) on agar plates were enumerated after incubation at 37 °C for 3 days.

Assessment of MSN Efficacy in Mice. Animal procedures were conducted according to protocols approved by the UCLA Animal Research Committee and NIH Guidelines for the Care and Use of Laboratory Animals in Research. In two experiments (Experiment 1 and Experiment 2), female Balb/c mice (Taconic) of approximately 18 g were provided with standard diet ad libitum and acclimated for one week. Mice were infected by the intranasal route with ~8000 (Experiment 1) or ~4000 (Experiment 2) CFU of *F. tularensis* LVS. Two mice were euthanized 5 hours after intranasal infection (day 0) to determine the number of bacteria delivered to the lung at the start of the experiment. An additional 3 mice were euthanized one day later (day 1) to determine bacterial growth during that period of time. Mice were then sham-treated or treated with MXF or MSN-MBI-MXF by tail vein injection every other day (day 1, day 3, and day 5) for a total of 3 treatments. Mice were euthanized one day after the last treatment (day 6). Lungs, livers, and spleens from infected mice that were sham-treated or treated with MXF or MSN-

MBI-MXF were homogenized and serially diluted for plating on GCII chocolate agar containing sulfamethoxazole (40 μg/mL), trimethoprim (8 μg/mL), and erythromycin (50 μg/mL). Bacterial CFU on the agar plates were enumerated after incubation at 37 °C for 4 days.

Median-Effect Plots. We used median-effect plots[35] to compare the relative efficacy of MSN-MBI-MXF and free MXF. The fraction of inhibition for samples treated with different amounts of MXF was calculated using bacterial CFU in base-10 logarithm (log CFU) with the equation: Fraction of inhibition = 1 - (log CFU from sample treated with MSN-MBI-MXF or MXF/log CFU from untreated sample). A median-effect plot for MSN-MBI-MXF or MXF was generated using MXF or MXF equivalent (MSNs) dose in base-10 logarithm as the X-axis and the fraction of surviving bacteria divided by the fraction of killed bacteria in base-10 logarithm as the Y-axis.

Statistics. Statistical analyses were performed using the Student's t-test. A *P* value of 0.05 or less was considered statistically significant.

ACKNOWLEDGMENTS

This work was supported by Defense Threat Reduction Agency Grant HDTRA1-13-1-0046. We thank Saša Masleša-Galić and Susana Nava for expert technical assistance and Angela Hwang, Philippe Saint-Cricq Riviere for helpful discussions and Bastian Ruehle for the TOC figure. The authors thank the Advanced Light Microscopy Facility in the UCLA/CNSI for providing confocal microscopy equipment.

Supporting Information Available: Additional release profile, DLS measurement, microscopy images, and characterization data. The Supporting Information is available free of charge on the ACS Publications website at http://pubs.acs.org.

FIGURES

TOC Graphic: Gated nanoparticles carry large quantities of moxifloxicin into macrophages, release the cargo and kill intracellular *F. tularensis* both in cultures and in mice.

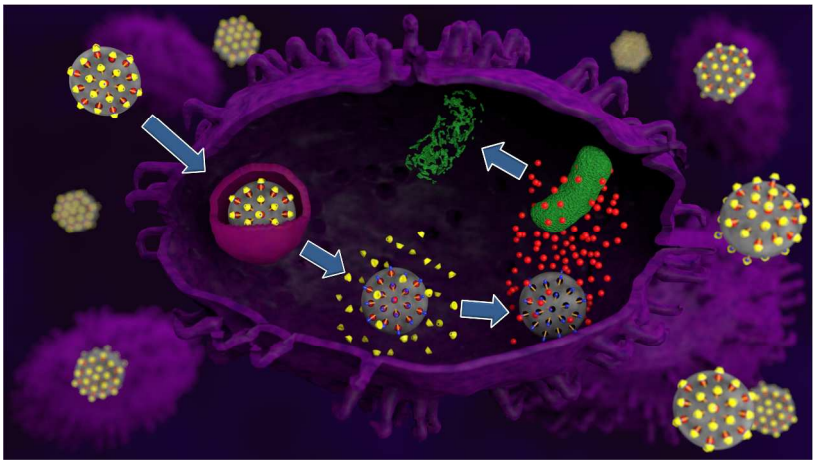

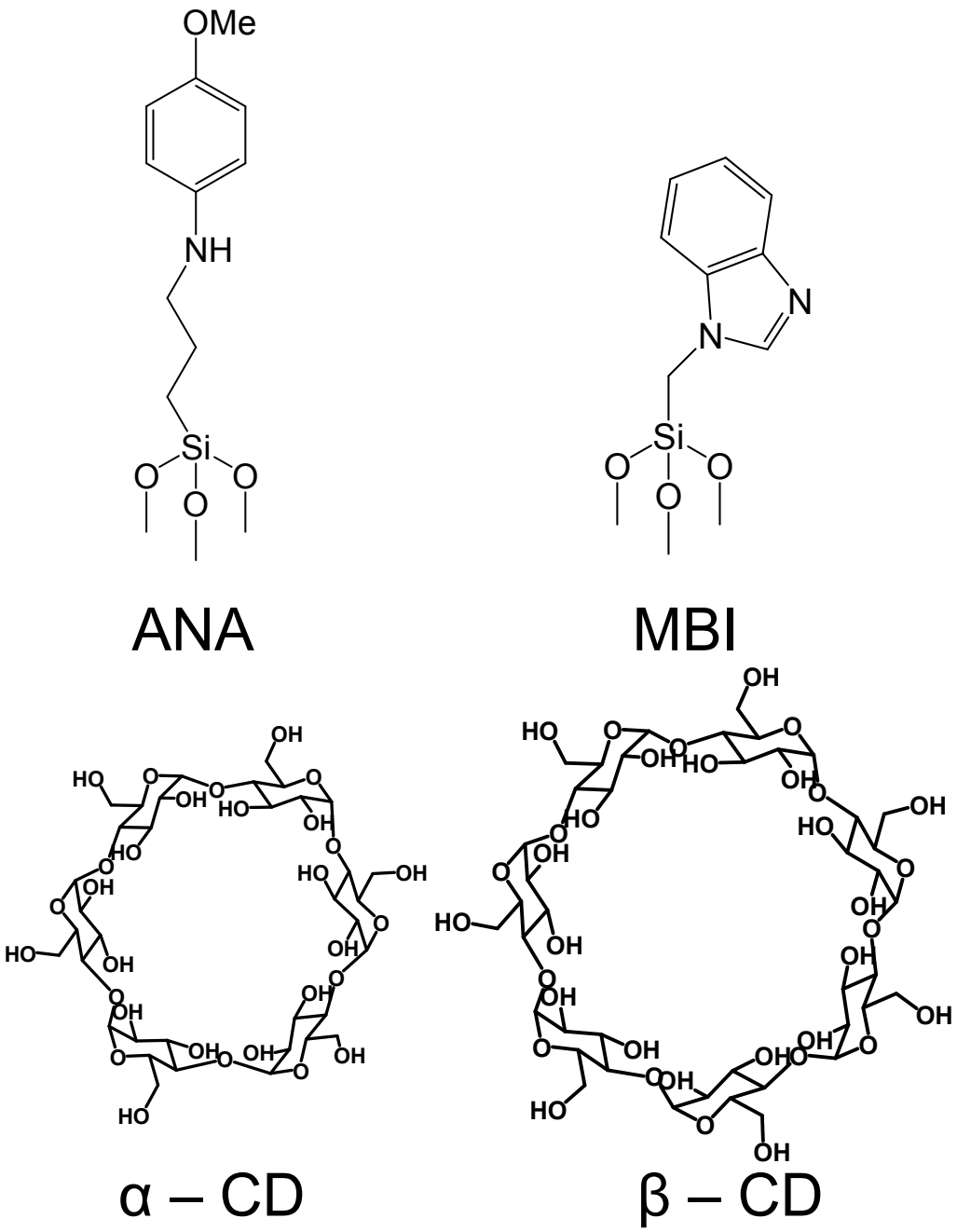

Figure 1. Chemical structures of the stalks (top) and caps (bottom) of two nanovalves. Left: the ANA (stalk) and α-CD (cap); Right: the MBI (stalk) and β-CD (cap)

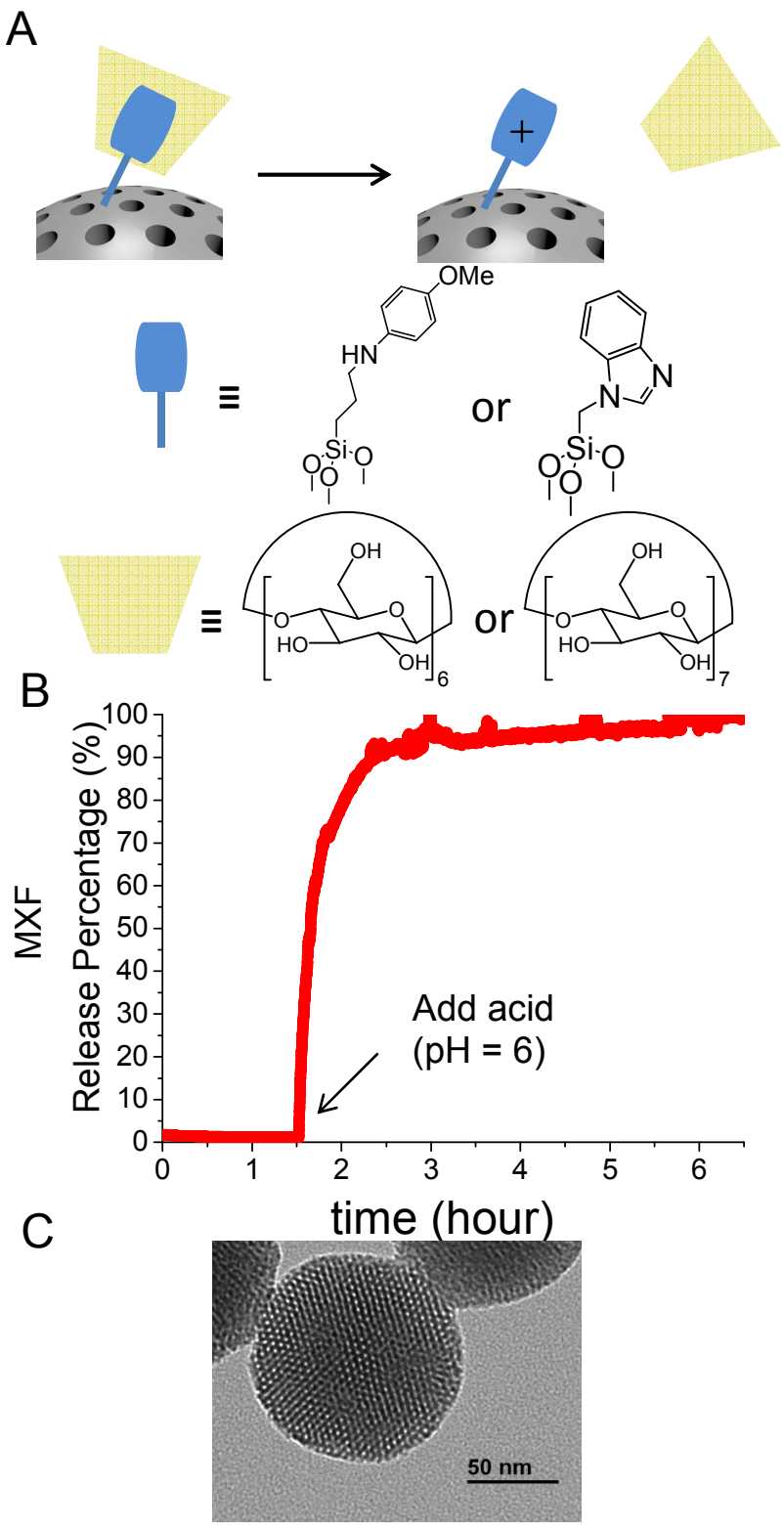
A
OMe
HN
Si
O
or
N
N
OH
HO
6
7
B
MXF
Release Percentage (%)
100
90
80
70
60
50
40
30
20
10
0
Add acid
(pH = 6)
0
1
2
3
4
5
6
time (hour)
C
50 nm

Figure 2. (A). Attachment of two different pH-sensitive nanovalves on MCM-41 surface. When the stalk is protonated, the cap molecule α-CD or β-CD dissociates from it due to the decrease of the binding constant between them. (B) MSN-MBI-MXF drug release profile. There is no leakage at pH 7, as indicated by the flat baseline; drug release starts when the pH is lowered to 6 by addition of acid. (C) TEM image of MCM-41 showing its hexagonal pore structure.

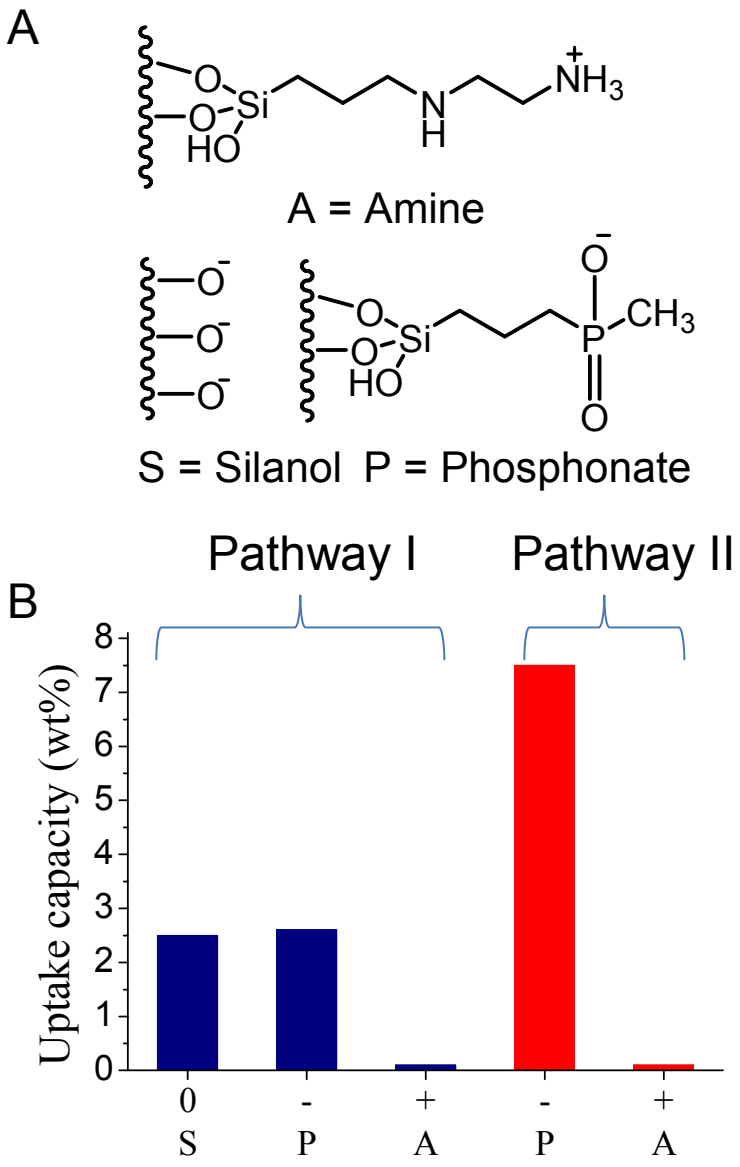

Figure 3. (A) Uptake capacity of MSN-MBI with different inner mesopore charges and stalk synthetic pathways. From left to right, samples are: slightly negatively charged underivatized MSN with stalk MBI synthesized by pathway I; negatively charged MSN-MBI by pathway I; positively charged MSN-MBI by pathway I; negatively charged MSN-MBI by pathway II; and positively charged MSN-MBI by pathway II. Pathyway I: synthesize the whole stalk first and then attach it on MCM-41; pathway II: attach first part of stalk on MCM-41 first and then

synthesize the whole stalk. Negatively charged MCM-41 with nanovalve-MBI, synthesized by pathway II has highest uptake capacity, and positively charged MCM-41 uptakes almost nothing. (B) MSN mesopores modified (left to right) with amine (+), unmodified silanol (-), or phosphonate (-).

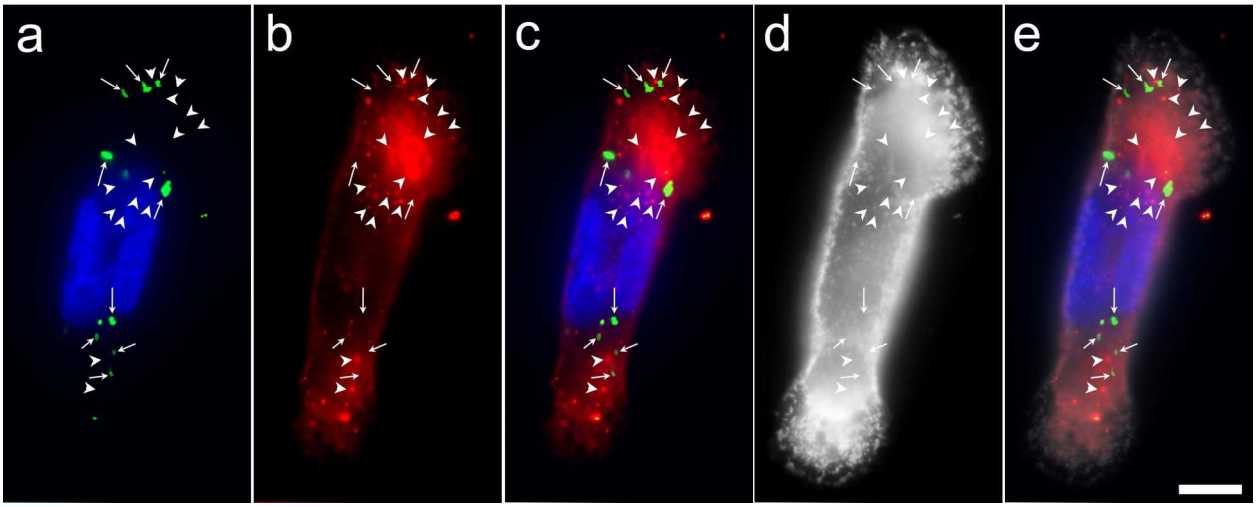

Figure 4. Confocal microscopy image of a *F. tularensis*- infected THP-1 macrophage that has taken up RITC-labeled MSN-MBI. Human macrophage-like THP-1 cells were infected with GFP-expressing *F. tularensis* for 90 min, washed, and incubated with 12.5 μg/mL of RITC-labeled 100 nm MSN-MBI. After 3 hours, the cells were washed; the plasma membrane was stained with WGA-AlexaFluor 633; the cells were fixed; and nuclei were stained with DAPI. (a) LVS-GFP (green, arrows) and DAPI-stained nucleus (blue); (b) RITC-labeled MSN-MBI (red, arrowheads); (c) merged red, green, and blue color image; (d) contours of the cell are stained with WGA-AlexaFluor 633 (gray scale); (e) gray scale image superimposed onto merged color image, with the WGA-AlexaFluor 633 gray scale channel made partially transparent to allow the other channels to be seen. Scale bars, 10 μm. The experiment was done twice with similar results.

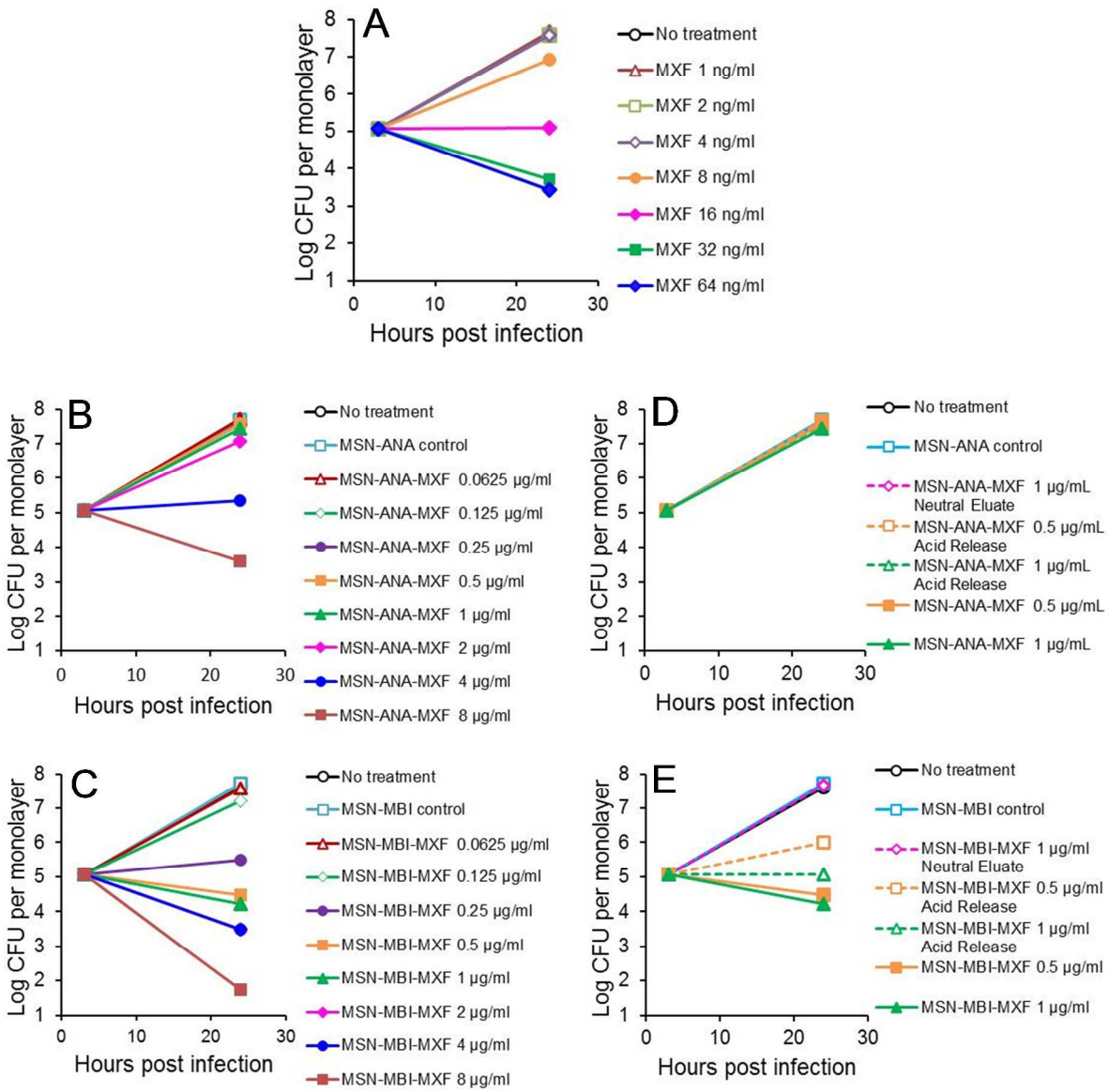

Figure 5. *In vitro* efficacy of MXF-loaded MSNs functionalized with two different types of pH-sensitive nanovalves. Human THP-1 macrophages were infected with *F. tularensis* LVS and treated with (A) MXF, (B) MSN-ANA-MXF or (C) MSN-MBI-MXF. Viable bacteria were determined by enumerating colony forming units (CFU) of *F. tularensis* in the macrophage monolayer. Impact of the drug released from (D) MSN-ANA-MXF and (E) MSN-MBI-MXF by maleate pH 1.8 was assessed in the infected macrophage bioassay. Data shown are means of triplicate platings per macrophage monolayer, n = 1.

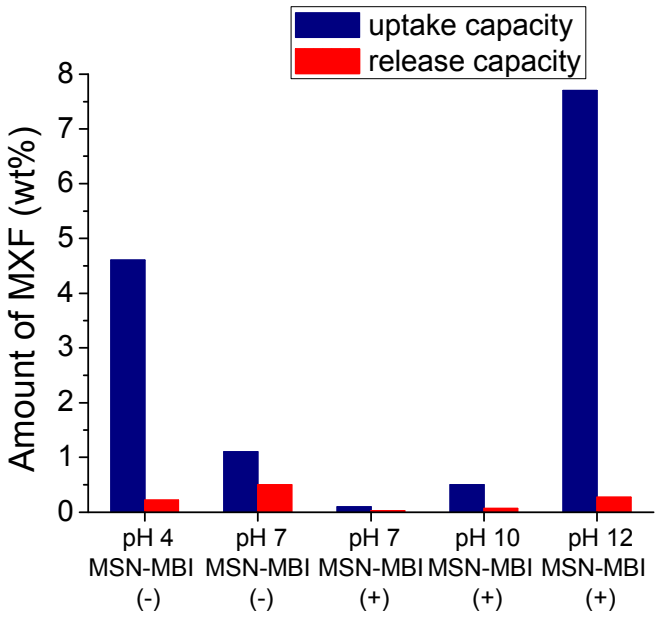

Figure 6. Uptake and release capacity of negatively charged MSN-MBI loaded at pH 4 or 7 and positively charged MSN-MBI loaded at pH 7, 10, or 12 MXF aqueous solution. MXF has positive net charge in solution at pH $\leqslant$ 7 and MCM-41 is negatively charged. Decreasing the loading pH from 7 to 4 increases uptake capacity, but, not release capacity because the nanovalve is open at pH 6 and particles must be transferred to neutral solution before capping. Most of MXF diffuses out of the pores because of these extra steps. At pH 7, positively charged MCM-41 repels MXF and leads to very low uptake and release capacities. MXF has negative charge when solution pH > 7, and increasing pH dramatically improves uptake capacities. However, loading at pH 12 does not lead to highest release capacity because particles degrade in base solution within 24 hours.

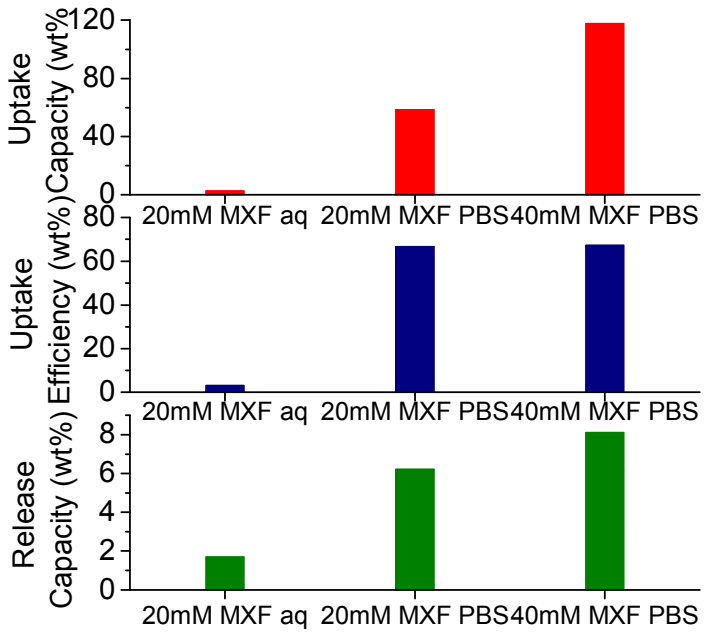

Figure 7. Uptake capacity, uptake efficiency and release capacity of phosphonated MSN-MBI loaded in 20 mM MXF aqueous solution (pH 7), 20 mM MXF PBS solution (pH 7.4) and 40 mM MXF PBS solution (pH 7.4). At same concentration 20 mM MXF, PBS loading increases the uptake more than 10 times than neutral water and release capacity got increased to 6.2 wt%, which is more than 3 times of 1.7 wt% from neutral loading. Increasing the loading concentration to 40 mM further improves uptake capacity to almost 120 wt% and release capacity 8.1 wt%. In terms of uptake efficiency, MSN-MBI uptakes around 70 % MXF from original solution for both 20 mM and 40 mM MXF loading.

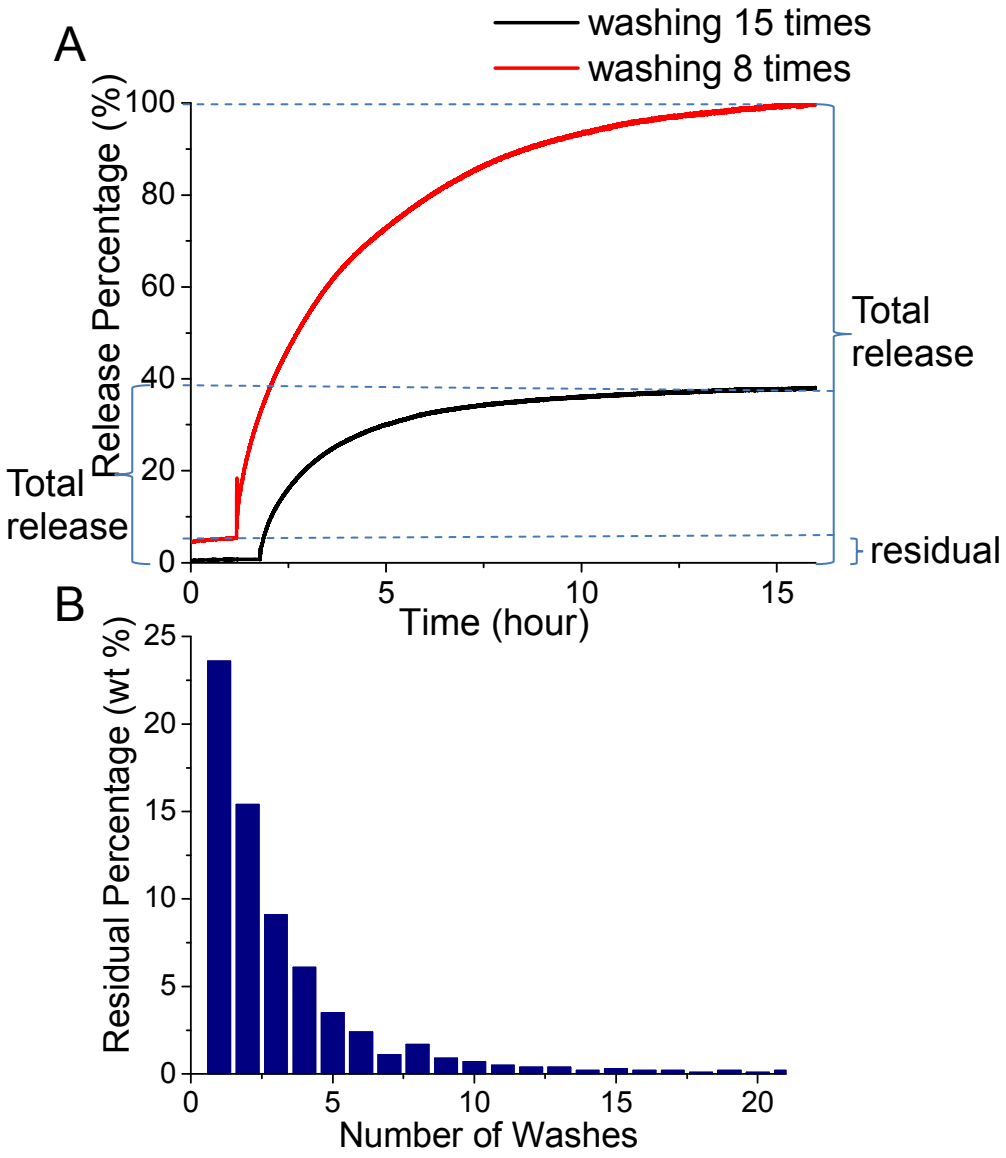

Figure 8. (A) Release profiles show that the more times the MSN are washed, the lower the amount of residual and release capacity. When particles were washed 15 times, there was negligible residual drug detected from the particle surface (no fluorescence detected). A small amount of residual was observed when drug loaded particles were washed 8 times. The experiments were repeated three times and all of them show the same relation between washing and release capacity. (B) The amount of MXF washed away each time decreases as the number

of washes increases; the decrease for each step is ~30 %. The first eight washes contribute ~95 % to the total amount of MXF ultimately removed by washing.

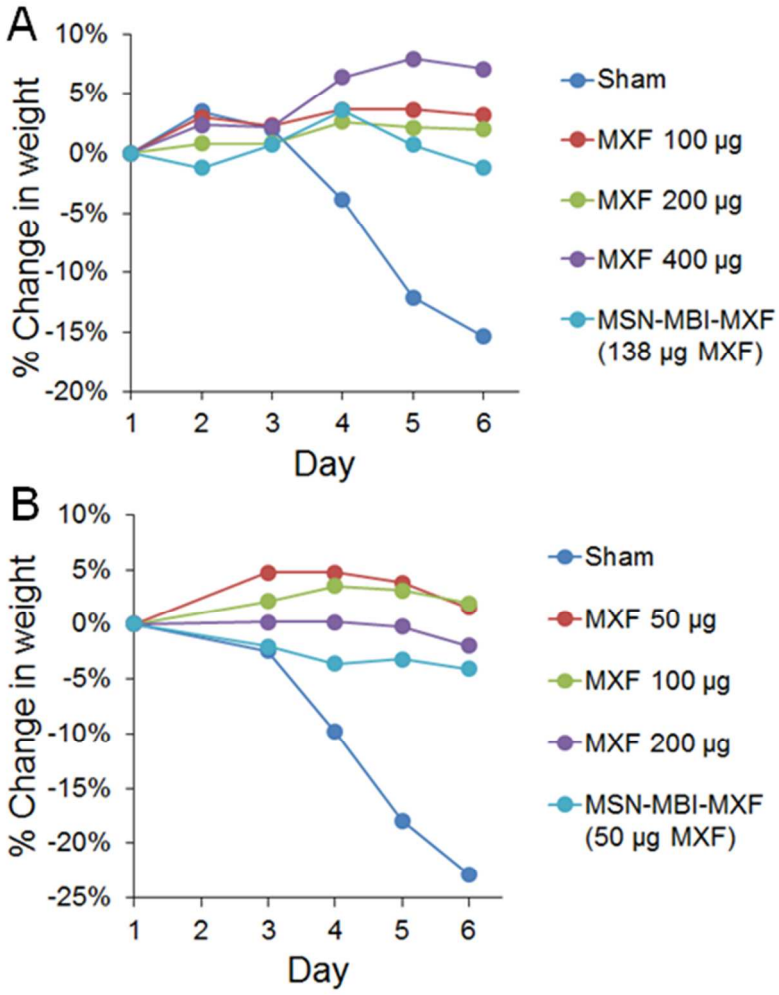

Figure 9. Treatment with MSN-MBI-MXF prevents weight loss caused by pneumonic tularemia. A and B show two independent mouse experiments (Experiment 1 and Experiment 2, respectively) in which the percentage change in weight of *F. tularensis*-infected mice was monitored over the course of the experiments. The mice were sham treated, treated with one of three doses of MXF as a free drug, as indicated, or treated with MSN-MBI-MXF (loaded with

138 µg MXF in Experiment 1 and 50 µg MXF in Experiment 2). Data shown are means of 3 – 4 mice per group. The experiment was done twice and both experiments are shown above.

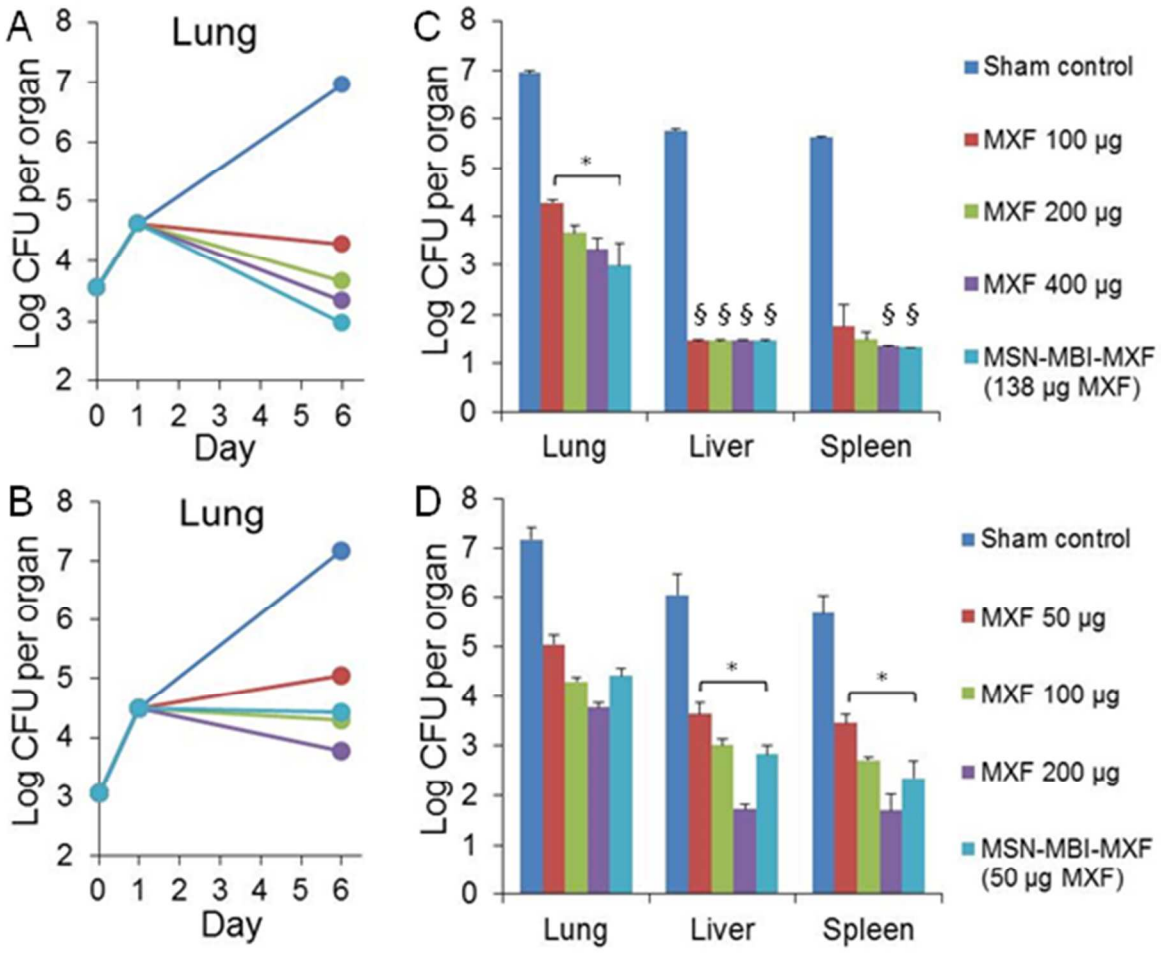

Figure 10. *In vivo* efficacy of MSN-MBI-MXF assessed by assay of *F. tularensis* burden in the mouse organs in two independent experiments, Experiment 1 (A and C) and Experiment 2 (B and D). Mice were infected with *F. tularensis* LVS by the intranasal route. (A and B) Bacterial burden in the lung was monitored over the course of infection. One day post-infection, mice were sham treated, treated with one of three doses of free MXF, as indicated, or treated with MSN-MBI-MXF (loaded with 138 µg in Experiment 1 shown in A and 50 µg in Experiment 2 shown in B) by tail vein injection on days 1, 3, and 5. (C and D) Mice were euthanized one day after the last dose of treatment (day 6) to enumerate bacterial numbers in the lung, liver, and

spleen. § Bacterial CFU below limit of detection. *P < 0.05 by one-tailed t-test. Data shown are means ± S.E. for 3 – 4 mice per group. The experiment was done twice and both experiments are shown above.

Table 1. MXF molecular species distribution under different pH

MXF	Species in solution (calculated ratio %)					
	Positively charged			Negatively Charged		
	pH 4	pH 7	pH 7.4	pH 8	pH 10	pH 12
$^{+}H_2N…COOH$	99.50	16.60	7.30	1.90	0.01	0.01
$^{+}H_2N…COO^{-}$	0.49	83.30	87.80	93.50	16.60	0.20
$HN…COO^{-}$	0.01	0.10	4.80	4.60	83.30	99.79

% fully protonated form ($^{+}H_2N…COOH$) = 100 / ($1+10^{pH\text{-}pKa1} + 10^{2*pH\text{-}pKa1\text{-}pKa2}$), % zwitterions ($^{+}H_2N…COOH^{-}$) = 100 / ($1+10^{pKa1\text{-}pH} + 10^{pH\text{-}pKa2}$), % fully deprotonated form ($HN…COOH^{-}$) = 100 - % ($^{+}H_2N…COOH$) - % ($^{+}H_2N…COOH^{-}$)[36]

Table 2. Uptake and release capacity of phosphonated MSN with pH sensitive nanovalves

Sample	Uptake capacity (wt %)	Release capacity (wt %)
MSN-ANA-MXF (α-CD cap)	2.8 %	0.16 %
MSN-MBI-MXF (β-CD cap)	7.4 %	1.02 %

Table 3. Uptake capacity of MXF loaded MSN with different nanovalves (at low concentration)

Sample	Uptake capacity (wt %)
MSN-ANA-MXF	20 %
MSN-MBI-MXF	51.4 %

REFERENCES

1. Ellis, J.; Oyston, P. C.; Green, M.; Titball, R. W. Tularemia. *Clin. Microbiol. Rev.* **2002,** *15*, 631-646.

2. Christopher, G. W.; Cieslak, T. J.; Pavlin, J. A.; Eitzen, E. M. Biological Warfare - A Historical Perspective. *Jama-J Am Med Assoc* **1997,** *278*, 412-417。

3. Harris, S. Japanese Biological Warfare Research on Humans - A Case-Study of Microbiology and Ethics. *Ann Ny Acad Sci* **1992,** *666*, 21-52.

4. Alibek, K.; Handelman, S. *Biohazard : the Chilling True Story of the Largest Covert Biological Weapons Program in the World, Told from the inside by the Man Who Ran It*. Random House: New York, 1999; pp 319.

5. Feldman, K. A.; Enscore, R. E.; Lathrop, S. L.; Matyas, B. T.; McGuill, M.; Schriefer, M. E.; Stiles-Enos, D.; Dennis, D. T.; Petersen, L. R.; Hayes, E. B. An Outbreak of Primary Pneumonic Tularemia on Martha's Vineyard. *New Engl J Med* **2001,** *345*, 1601-1606.

6. Chocarro, A.; Gonzalez, A.; Carcia, I. Treatment of Tularemia with Ciprofloxacin. *Clin Infect Dis* **2000,** *31*, 623-623.

7. Chen, H. W.; Wang, L. Y.; Yeh, J.; Wu, X. Y.; Cao, Z. H.; Wang, Y. A.; Zhang, M. M.; Yang, L.; Mao, H. Reducing Non-Specific Binding and Uptake of Nanoparticles and Improving Cell Targeting with An Antifouling PEO-b-P Gamma MPS Copolymer Coating. *Biomaterials* **2010,** *31*, 5397-5407.

8. Lee, J. E.; Lee, N.; Kim, H.; Kim, J.; Choi, S. H.; Kim, J. H.; Kim, T.; Song, I. C.; Park, S. P.; Moon, W. K.; *et al*. Uniform Mesoporous Dye-Doped Silica Nanoparticles Decorated with

Multiple Magnetite Nanocrystals for Simultaneous Enhanced Magnetic Resonance Imaging, Fluorescence Imaging, and Drug Delivery. *J Am Chem Soc* **2010,** *132*, 552-557.

9. He, Q. J.; Zhang, Z. W.; Gao, F.; Li, Y. P.; Shi, J. L. *In vivo* Biodistribution and Urinary Excretion of Mesoporous Silica Nanoparticles: Effects of Particle Size and PEGylation. *Small* **2011,** *7*, 271-280.

10. Barbe, C.; Bartlett, J.; Kong, L. G.; Finnie, K.; Lin, H. Q.; Larkin, M.; Calleja, S.; Bush, A.; Calleja, G. Silica particles: A Novel Drug-Delivery System. *Adv Mater* **2004,** *16*, 1959-1966.

11. Argyo, C.; Weiss, V.; Brauchle, C.; Bein, T. Multifunctional Mesoporous Silica Nanoparticles as A Universal Platform for Drug Delivery. *Chem Mater* **2014,** *26*, 435-451.

12. Li, Z. X.; Barnes, J. C.; Bosoy, A.; Stoddart, J. F.; Zink, J. I. Mesoporous Silica Nanoparticles in Biomedical Applications. *Chem Soc Rev* **2012,** *41*, 2590-2605.

13. Tarn, D.; Ashley, C. E.; Xue, M.; Carnes, E. C.; Zink, J. I.; Brinker, C. J. Mesoporous Silica Nanoparticle Nanocarriers: Biofunctionality and Biocompatibility. *Accounts Chem Res* **2013,** *46*, 792-801.

14. Xue, M.; Zhong, X.; Shaposhnik, Z.; Qu, Y. Q.; Tamanoi, F.; Duan, X. F.; Zink, J. I. pH-Operated Mechanized Porous Silicon Nanoparticles. *J Am Chem Soc* **2011,** *133*, 8798-8801.

15. Meng, H. A.; Xue, M.; Xia, T. A.; Zhao, Y. L.; Tamanoi, F.; Stoddart, J. F.; Zink, J. I.; Nel, A. E. Autonomous *In vitro* Anticancer Drug Release from Mesoporous Silica Nanoparticles by pH-Sensitive Nanovalves. *J Am Chem Soc* **2010,** *132*, 12690-12697.

16. Hwang, A. A.; Lu, J.; Tamanoi, F.; Zink, J. I. Functional Nanovalves on Protein-Coated Nanoparticles for *In vitro* and *In vivo* Controlled Drug Delivery. *Small* **2015,** *11*, 319-328.

17. Dong, J. Y.; Xue, M.; Zink, J. I. Functioning of Nanovalves on Polymer Coated Mesoporous Silica Nanoparticles. *Nanoscale* **2013,** *5*, 10300-10306.

18. Ferris, D. P.; Zhao, Y. L.; Khashab, N. M.; Khatib, H. A.; Stoddart, J. F.; Zink, J. I. Light-Operated Mechanized Nanoparticles. *J. Am. Chem. Soc.* **2009,** *131*, 1686-1688.

19. Thomas, C. R.; Ferris, D. P.; Lee, J. H.; Choi, E.; Cho, M. H.; Kim, E. S.; Stoddart, J. F.; Shin, J. S.; Cheon, J.; Zink, J. I. Noninvasive Remote-Controlled Release of Drug Molecules *In vitro* Using Magnetic Actuation of Mechanized Nanoparticles. *J Am Chem Soc* **2010,** *132*, 10623-10625.

20. Clemens, D. L.; Lee, B. Y.; Xue, M.; Thomas, C. R.; Meng, H.; Ferris, D.; Nel, A. E.; Zink, J. I.; Horwitz, M. A. Targeted Intracellular Delivery of Antituberculosis Drugs to Mycobacterium Tuberculosis-Infected Macrophages *via* Functionalized Mesoporous Silica Nanoparticles. *Antimicrob Agents Ch* **2012,** *56*, 2535-2545.

21. Liong, M.; Lu, J.; Kovochich, M.; Xia, T.; Ruehm, S. G.; Nel, A. E.; Tamanoi, F.; Zink, J. I. Multifunctional Inorganic Nanoparticles for Imaging, Targeting, and Drug Delivery. *ACS Nano* **2008,** *2*, 889-896.

22. Luo, G. F.; Chen, W. H.; Liu, Y.; Lei, Q.; Zhuo, R. X.; Zhang, X. Z. Multifunctional Enveloped Mesoporous Silica Nanoparticles for Subcellular Co-Delivery of Drug and Therapeutic Peptide. *Scientific reports* **2014,** *4*, 6064.

23. Lu, J.; Liong, M.; Li, Z. X.; Zink, J. I.; Tamanoi, F. Biocompatibility, Biodistribution, and Drug-Delivery Efficiency of Mesoporous Silica Nanoparticles for Cancer Therapy in Animals. *Small* **2010,** *6* , 1794-1805.

24. Steward, J.; Piercy, I.; Lever, M. S.; Simpson, A. J. H.; Brooks, T. J. G. Treatment of Murine Pneumonic *Francisella tularensis* Infection with Gatifloxacin, Moxifloxacin or Ciprofloxacin. *Int J Antimicrob Ag* **2006,** *27*, 439-443.

25. Du, L.; Liao, S. J.; Khatib, H. A.; Stoddart, J. F.; Zink, J. I. Controlled-Access Hollow Mechanized Silica Nanocontainers. *J Am Chem Soc* **2009,** *131*, 15136-15142.

26. Clemens, D. L.; Lee, B. Y.; Horwitz, M. A. Virulent and Avirulent Strains of *Francisella tularensis* Prevent Acidification and Maturation of Their Phagosomes and Escape into the Cytoplasm in Human Macrophages. *Infect. Immun.* **2004,** *72*, 3204-3217.

27. Meng, H.; Liong, M.; Xia, T.; Li, Z.; Ji, Z.; Zink, J. I.; Nel, A. E. Engineered Design of Mesoporous Silica Nanoparticles to Deliver Doxorubicin and P-glycoprotein siRNA to Overcome Drug Resistance in A Cancer Cell Line. *ACS Nano* **2010,** *4*, 4539-4550.

28. Storm, G.; Belliot, S. O.; Daemen, T.; Lasic, D. D. Surface Modification of Nanoparticles to Oppose Uptake by the Mononuclear Phagocyte System. *Adv. Drug Del. Rev.* **1995,** *17*, 31-48.

29. Clemens, D. L.; Lee, B. Y.; Horwitz, M. A. O-Antigen-Deficient *Francisella tularensis* Live Vaccine Strain Mutants are Ingested *via* An Aberrant Form of Looping Phagocytosis and Show Altered Kinetics of Intracellular Trafficking in Human Macrophages. *Infect Immun* **2012,** *80*, 952-967.

30. Ilinskaya, A. N.; Dobrovolskaia, M. A. Nanoparticles and the Blood Coagulation System. Part II: Safety Concerns. *Nanomedicine (Lond)* **2013,** *8*, 969-981.

31. Fornaguera, C.; Caldero, G.; Mitjans, M.; Vinardell, M. P.; Solans, C.; Vauthier, C. Interactions of PLGA Nanoparticles with Blood Components: Protein Adsorption, Coagulation, Activation of the Complement System and Hemolysis Studies. *Nanoscale* **2015,** *7*, 6045-6058.

32. Nel, A.; Xia, T.; Madler, L.; Li, N. Toxic Potential of Materials at the Nanolevel. *Science* **2006,** *311*, 622-627.

33. Jia, Q. M.; Lee, B. Y.; Bowen, R.; Dillon, B. J.; Som, S. M.; Horwitz, M. A. A *Francisella tularensis* Live Vaccine Strain (LVS) Mutant with A Deletion in capB, Encoding A Putative Capsular Biosynthesis Protein, is Significantly More Attenuated than LVS Yet Induces Potent Protective Immunity in Mice against *F. tularensis* Challenge. *Infect Immun* **2010,** *78*, 4341-4355.

34. Jia, Q. M.; Lee, B. Y.; Clemens, D. L.; Bowen, R. A.; Horwitz, M. A. Recombinant Attenuated Listeria Monocytogenes Vaccine Expressing *Francisella tularensis* IglC Induces Protection in Mice against Aerosolized Type A *F. tularensis*. *Vaccine* **2009,** *27*, 1216-1229.

35. Chou, T. C. Theoretical Basis, Experimental Design, and Computerized Simulation of Synergism and Antagonism in Drug Combination Studies. *Pharmacol Rev* **2006,** *58*, 621-681.

36. Lemaire, S.; Tulkens, P. M.; Van Bambeke, F. Contrasting Effects of Acidic pH on the Extracellular and Intracellular Activities of the Anti-Gram-Positive Fluoroquinolones Moxifloxacin and Delafloxacin against Staphylococcus Aureus. *Antimicrob Agents Ch* **2011,** *55*, 649-658.

Supporting Information

Mesoporous Silica Nanoparticles with pH – Sensitive Nanovalves for Delivery of Moxifloxacin Provide Improved Treatment of Lethal Pneumonic Tularemia

Zilu Li[1,3,#], *Daniel L. Clemens*[2,#], *Bai-Yu Lee*[2,#], *Barbara Jane Dillon*[2], *Marcus A. Horwitz*[2,*] *Jeffrey I. Zink*[3,4,*]

[1]Department of Materials Science and Engineering

[2]Division of Infectious Diseases, Department of Medicine

[3]Department of Chemistry & Biochemistry

[4]California NanoSystems Institute,

University of California, Los Angeles, California, USA

[#] Z. Li, D. L. Clemens, and B.-Y. Lee contributed equally

Address correspondence to Marcus A. Horwitz, Dept. of Medicine, CHS 37-121, UCLA School of Medicine, 10833 Le Conte Ave., Los Angeles, CA 90095-1688, USA. Phone: (310) 206-0074; Fax: (310) 794-7156; E-mail: mhorwitz@mednet.ucla.edu. or to Jeffrey I. Zink, Dept. of Chemistry and Biochemistry, UCLA, 3013 Young Dr. East, Los Angeles, CA 90095-1569, USA. Phone: (310) 825-1001; Fax: (310) 825-4911; E-mail: jiz@chem.ucla.edu.

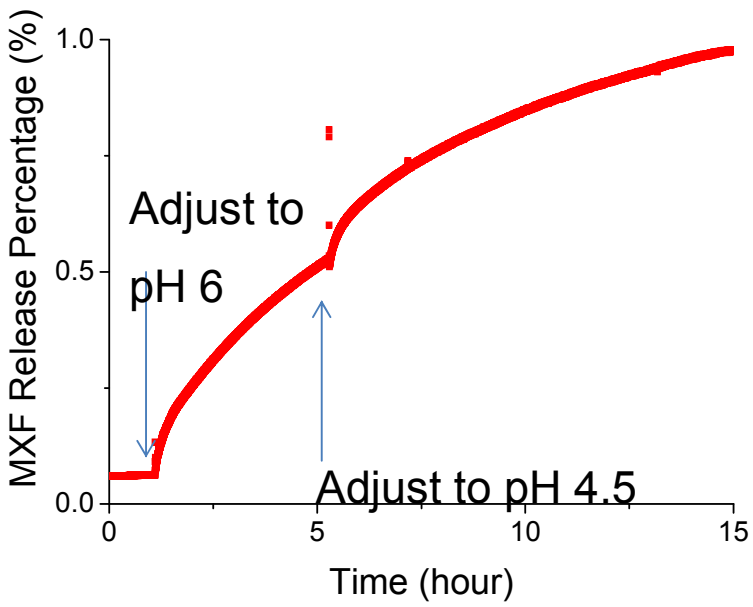

Figure S1. MSN-MBI-MXF release profile. There is no leakage at pH 7 evidenced by the flat baseline. Drug release starts at when the pH is lower than 6. The release rate can be further increased by lowering pH to 4.5.

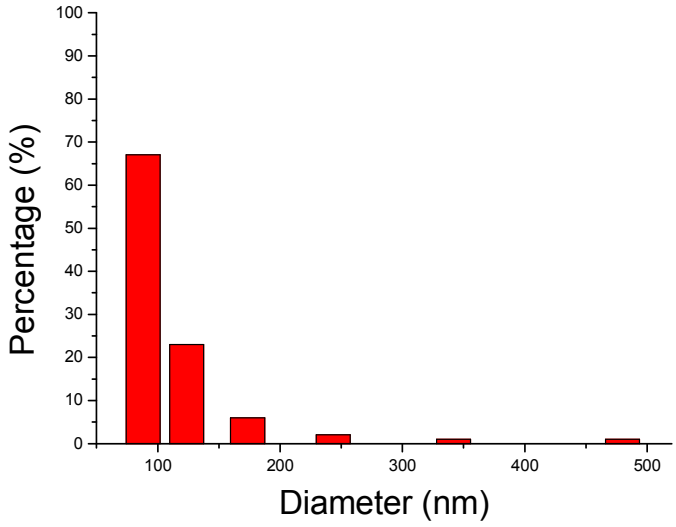

Figure S2. Dynamic light scattering (DLS) measurement of MSN with pH sensitive nanovalve. The mean hydrodynamic diameter of the modified nanoparticle is around 100 nm.

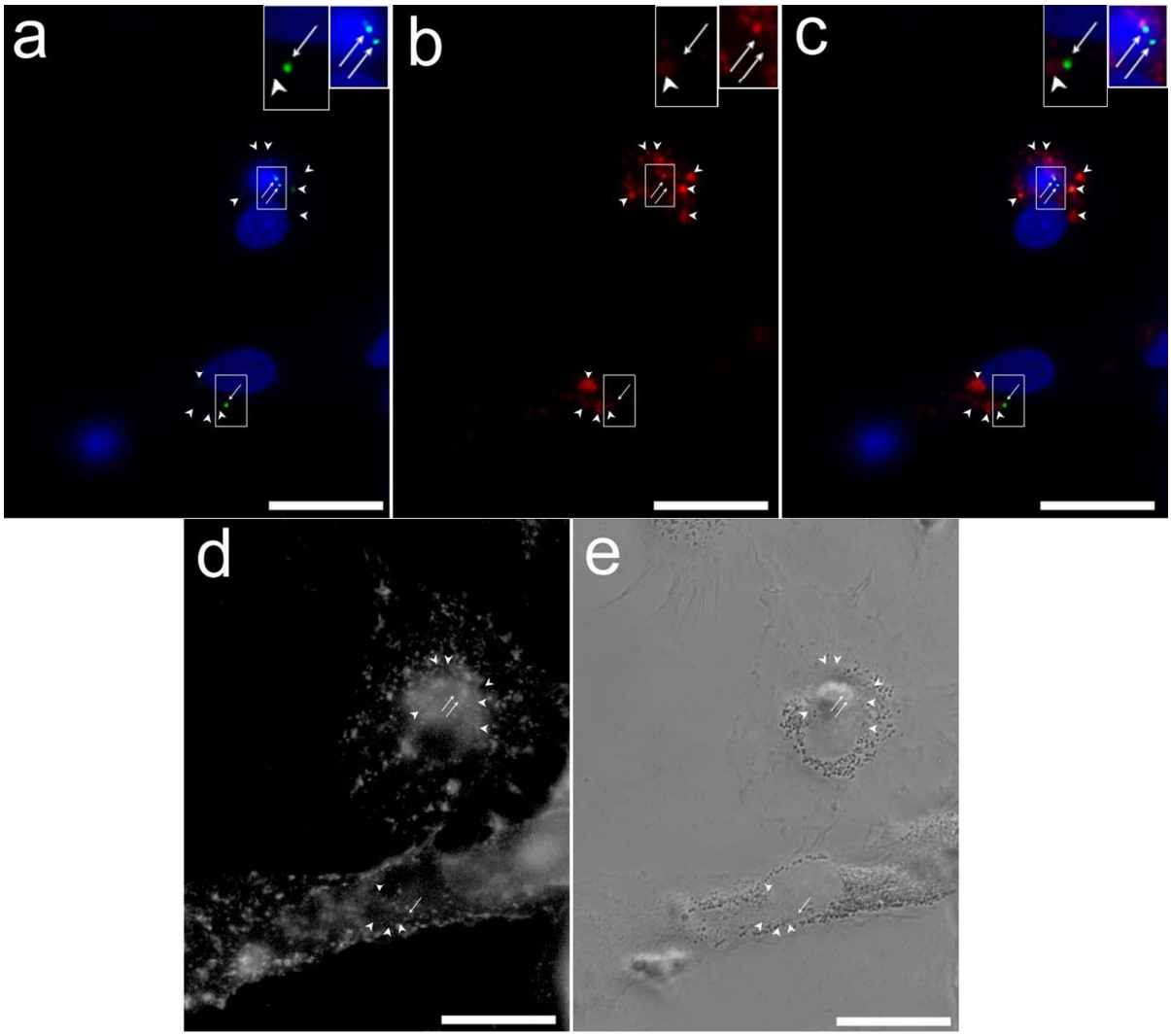

Figure S3. Epifluorescence and phase contrast microscopy demonstrates uptake of RITC-labeled MSN-MBI by *F. tularensis*-infected human monocyte derived macrophages (MDM). Human MDM cells were infected with GFP-expressing *F. tularensis* for 90 min, washed, and incubated with 12.5 μg/mL of RITC-labeled 100 nm MSN-MBI. After 3 hours, the cells were washed; the plasma membrane was stained with WGA-AlexaFluor 633; the cells were fixed; and nuclei were stained with DAPI. (a) LVS-GFP (green, arrows) and DAPI-stained nucleus (blue); (b) RITC-labeled MSN-MBI (red, arrowheads); (c) merged red, green, and blue color

image; (d) contours of the cell are stained with WGA-AlexaFluor 633 (gray scale); (e) phase contrast image. Scale bars, 10 μm. Boxed areas with arrows indicating locations of green fluorescent bacteria are shown at 2-fold higher magnification in the insets in the upper right of panels (a) – (c). The two bacteria overlying the DAPI stained nucleus appear turquoise rather than green because of merging of the blue and green channels. The experiment was done twice with similar results.

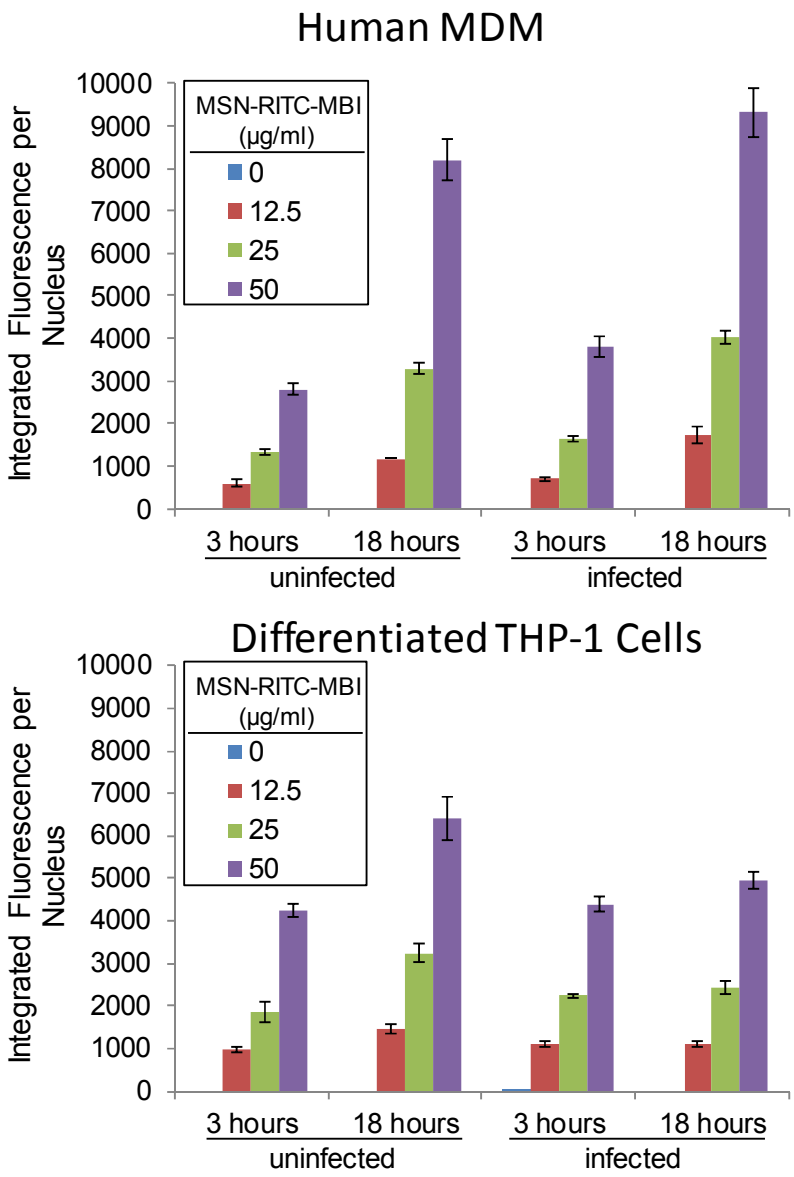

Figure S4. Quantitation of uptake of MSN-RITC-MBI by infected and uninfected human MDM and differentiated THP-1 cells. Uninfected or LVS-GFP infected human MDM (top panel) or THP-1 cells (bottom panel) were incubated with 0, 12.5, 25, or 50 µg/ml of MSN-RITC-MBI for 3 hours or 18 hours prior to staining and fixation as described in Figure S3. Automated high content imaging was performed with an ImageXpress robotic fluorescence microscope and MSN-RITC-MBI

integrated fluorescence intensity per DAPI-stained nucleus was quantitated using the granularity module of MetaXpress software. Data shown represent the means ± S.E. of duplicate wells (Human MDM) or of quadruplicate wells (THP-1 cells). The experiment was performed twice with similar results.

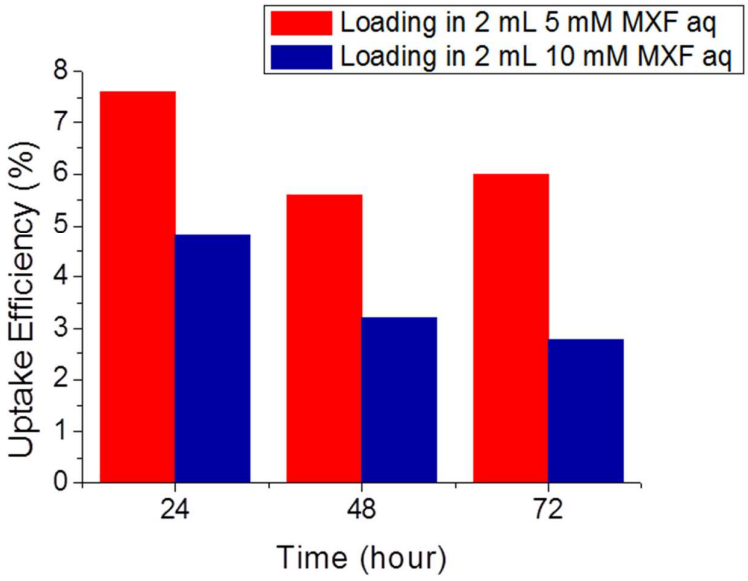

Figure S5. Uptake efficiency of MSN-MBI-MXF loading with 5 mM and 10 mM MXF aqueous solution for 24, 48 and 72 hours. 24 hours loading yielded the highest uptake efficiency for both low and high MXF concentrations.

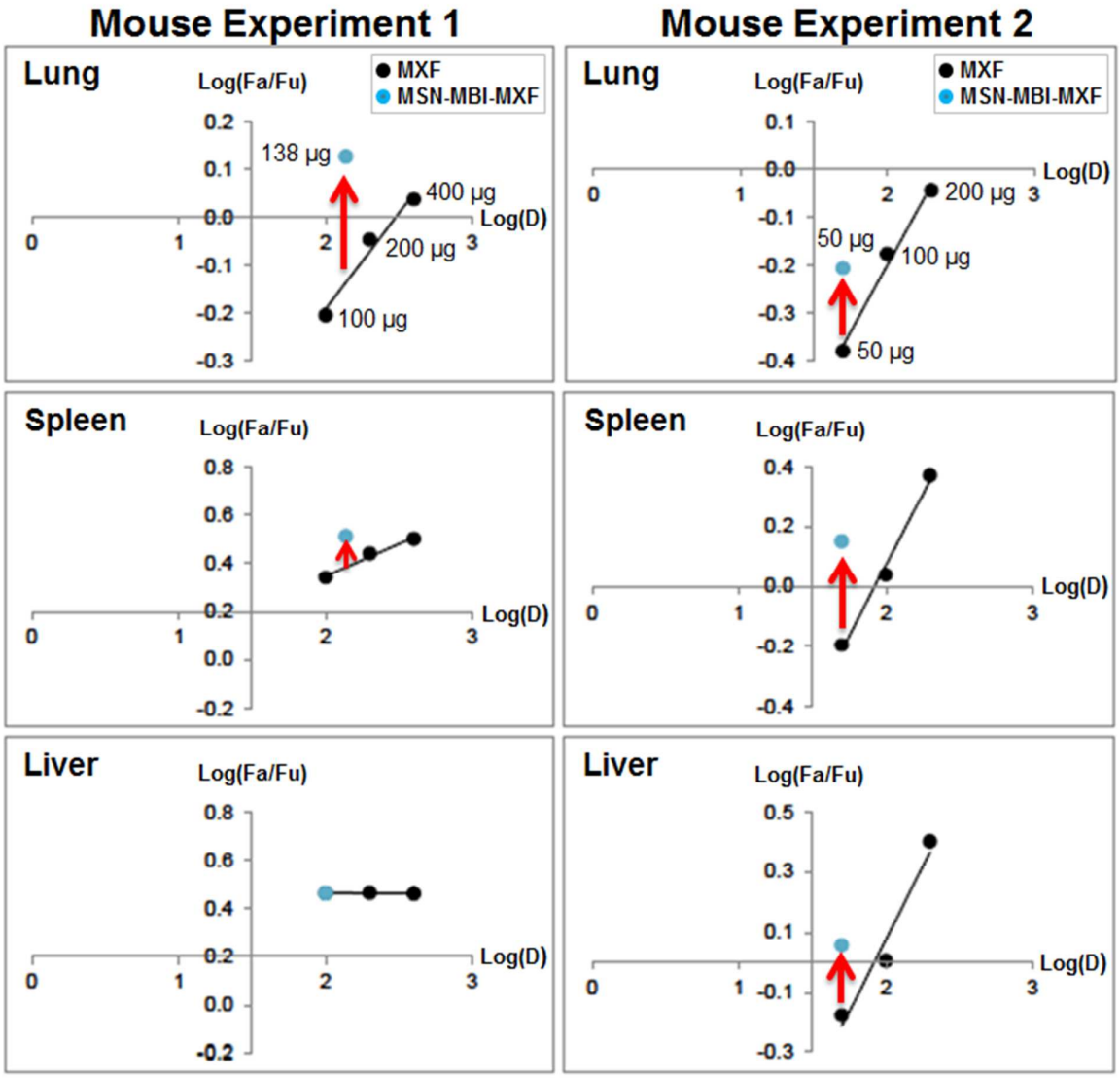

Figure S6. Median-effect plots to compare efficacy of MSN-MBI-MXF with MXF administered as free drug. The efficacy of MSN-MBI-MXF in the lung, spleen, and liver was compared with that of free MXF in a median-effect plot of the results of mouse Experiments 1 and 2. For a given dose of MXF, an upward shift as indicated by the red arrows on the y-axis indicates greater *F. tularensis* killing efficacy of the MSN-MBI-MXF. Fa: Fraction of bacteria killed; Fu: Fraction of bacteria surviving; D: Dose of MXF in micrograms.

Table S1. Bacterial CFU in infected macrophages with and without treatment

Condition	MXF amount	Duration	Log CFU
No treatment	0 ng/ml	3 hours	5.06
No treatment	0 ng/ml	1 day	7.60
MXF	1 ng/ml	1 day	7.65
MXF	2 ng/ml	1 day	7.59
MXF	4 ng/ml	1 day	7.59
MXF	8 ng/ml	1 day	6.92
MXF	16 ng/ml	1 day	5.09
MXF	32 ng/ml	1 day	3.72
MXF	64 ng/ml	1 day	3.43
MSN-MBI control (8 μg/ml)	0 ng/ml	1 day	7.72
MSN-MBI-MXF (0.0625 μg/ml)	1.65 ng/ml	1 day	7.59
MSN-MBI-MXF (0.125 μg/ml)	3.3 ng/ml	1 day	7.21
MSN-MBI-MXF (0.25 μg/ml)	6.6 ng/ml	1 day	5.49
MSN-MBI-MXF (0.5 μg/ml)	13.2 ng/ml	1 day	4.49
MSN-MBI-MXF (1 μg/ml)	26.4 ng/ml	1 day	4.23
MSN-MBI-MXF (2 μg/ml)	52.8 ng/ml	1 day	3.49
MSN-MBI-MXF (4 μg/ml)	105.6 ng/ml	1 day	3.49
MSN-MBI-MXF (8 μg/ml)	211.2 ng/ml	1 day	1.73
MSN-ANA control (8 μg/ml)	0 ng/ml	1 day	7.70
MSN-ANA-MXF (0.0625 μg/ml)	0.23 ng/ml	1 day	7.71
MSN-ANA-MXF (0.125 μg/ml)	0.45 ng/ml	1 day	7.72
MSN-ANA-MXF (0.25 μg/ml)	0.9 ng/ml	1 day	7.59
MSN-ANA-MXF (0.5 μg/ml)	1.8 ng/ml	1 day	7.59
MSN-ANA-MXF (1 μg/ml)	3.6 ng/ml	1 day	7.43
MSN-ANA-MXF (2 μg/ml)	7.2 ng/ml	1 day	7.06
MSN-ANA-MXF (4 μg/ml)	14.4 ng/ml	1 day	5.34
MSN-ANA-MXF (8 μg/ml)	28.8 ng/ml	1 day	3.61